THE ANTENNA LABORATORY

UNPUBLISHED PRELIMINARY DATA

RESEARCH ACTIVITIES in ---

Automatic Controls — *Antennas* — *Echo Area Studies*
Microwave Circuits — *Astronautics* — *E M Field Theory*
Terrain Investigations — *Radomes* — *Systems Analysis*
Wave Propagation — *Submillimeter Applications*

Radiation Patterns of Four Symmetrically Located Sources on a Perfectly Conducting Sphere

by

Li-jen Du and C. T. Tai

Grant Number NsG-448

1691-10 15 December 1964

Prepared for:
National Aeronautics and Space Administration
Office of Grants and Research Contracts
Washington, D. C. 20546

Department of ELECTRICAL ENGINEERING

THE OHIO STATE UNIVERSITY
RESEARCH FOUNDATION
Columbus, Ohio

REPORT 1691-10

REPORT

by

THE OHIO STATE UNIVERSITY RESEARCH FOUNDATION

COLUMBUS, OHIO 43212

Sponsor	National Aeronautics and Space Administration Office of Grants and Research Contracts Washington, D. C. 20546
Grant Number	NsG-448
Investigation of	Spacecraft Antenna Problems
Subject of Report	Radiation Patterns of Four Symmetrically Located Sources on a Perfectly Conducting Sphere
Submitted by	Li-jen Du and C. T. Tai Antenna Laboratory Department of Electrical Engineering
Date	15 December 1964

CONTENTS

RADIATION PATTERNS OF FOUR SYMMETRICALLY LOCATED SOURCES ON A PERFECTLY CONDUCTING SPHERE

Introduction

23947

In this report the radiation patterns of four symmetrically located sources (dipoles or small apertures) on a perfectly conducting sphere are presented. Analytical solutions are given which were programmed for the digital computer. The purpose of this investigation is to get some idea of the radiation field of a symmetrical antenna system mounted on a satellite which may be considered as a sphere. The data contained in this report may serve as a guide in selecting certain desirable patterns which can be obtained by varying such factors as the size of the sphere and the number of the sources, their positions on the sphere, and their relative magnitudes and phases.

author

The Dyadic Green's Function Pertaining to Exterior Problems of a Perfectly Conducting Sphere

For harmonically oscillating field with a time dependence of $e^{-i\omega t}$ the electric field vector E satisfies the differential equation

$$(1) \qquad \nabla \times \nabla \times \vec{E} - k^2 \vec{E} = i\omega\mu\vec{J},$$

where $k = 2\pi/\lambda$ and λ is the free space wavelength. Equation (1) can be integrated in a very compact manner by introducing a dyadic Green's function[1] which is a solution of the equation

$$(2) \qquad \nabla \times \nabla \times \overleftrightarrow{G}_e - k^2 \overleftrightarrow{G}_e = \overleftrightarrow{I}\, \delta(\vec{R}|\vec{R}'),$$

where $\overleftrightarrow{I}$ denotes the unit dyadic and $\delta(\vec{R}|\vec{R}')$ the three-dimensional delta function. Application of Green's theorem to $\vec{E}$ and $\overleftrightarrow{G}_e$ in a closed region yields the following equation:

$$(3)\qquad \vec{E} = i\omega\mu \iiint (\vec{J}' \cdot \overleftrightarrow{G}_e)dv' + \iint_S \left[(\vec{E}' \times \hat{n}) \cdot \nabla' \times \overleftrightarrow{G}_e + (\nabla' \times \vec{E}')(\hat{n} \times \overleftrightarrow{G}_e)\right] ds' .$$

In dealing with radiating current elements in the presence of a diffracting body, the surface of integration S occurring in the above equation can be chosen to be a composite surface consisting of the surface of the body S_d and a large sphere S_∞ at infinity. Because of the Sommerfeld radiation condition the surface integral over S_∞ vanishes and the second term in the surface integral can be eliminated if we require that $\overleftrightarrow{G}_e$ satisfies the following boundary condition on S_d:

$$(4)\qquad \hat{n} \times \overleftrightarrow{G}_e = 0.$$

Knowing $\overleftrightarrow{G}_e$ one can find the field due to a given current distribution, or the field due to apertures on a perfectly conducting body, by evaluating the integrals

$$(5)\qquad \vec{E} = i\omega\mu \iiint (\vec{J}' \cdot \overleftrightarrow{G}_e)dv'$$

or

$$(6)\qquad \vec{E} = \iint_{\text{aperture}} \left[(\vec{E}' \times \hat{n}) \cdot \nabla' \times \overleftrightarrow{G}_e\right] ds' .$$

The dyadic Green's function for a sphere, as derived in Reference 2, for the configuration shown in Fig. 1 is

$$(7)\qquad \overleftrightarrow{G}_e = \frac{ik}{4\pi} \sum_{n=1}^{\infty} \sum_{m=0}^{n} (2-\delta_o) \frac{2n+1}{n(n+1)} \cdot \frac{(n-m)!}{(n+m)!} \left\{ \left[\vec{M}'^{(1)}_{e_{omn}} + \alpha_n \vec{M}'^{(3)}_{e_{omn}} \right] \vec{M}^{(3)}_{e_{omn}} + \left[\vec{N}'^{(1)}_{e_{omn}} + \beta_n \vec{N}'^{(3)}_{e_{omn}} \right] \vec{N}^{(3)}_{e_{omn}} \right\} r > r',$$

where (R, θ, ϕ) = spherical coordinates of point of observation,
(R', θ', ϕ') = spherical coordinates of the source point,
a = radius of the sphere with center at origin,

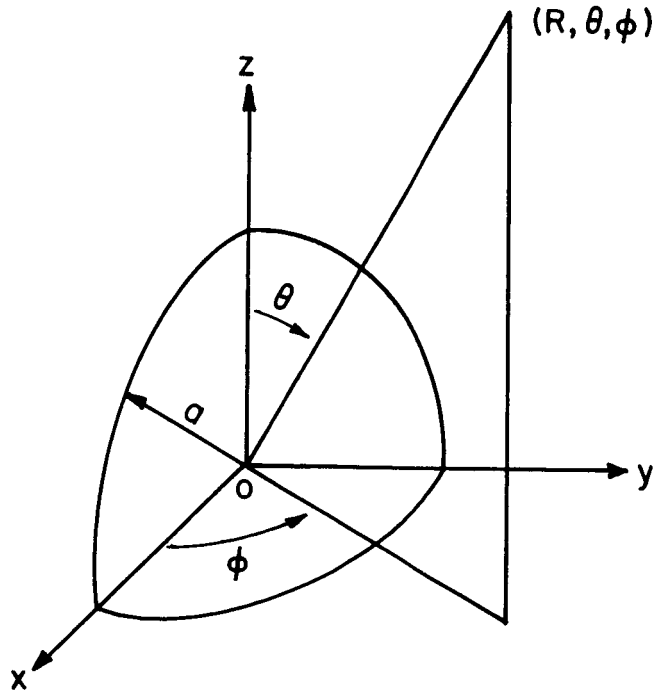

Fig. 1.

$$\psi_{\substack{e\\o}mn} = \begin{cases} \psi^{(1)}_{\substack{e\\o}mn} = j_n(kR) P_n^m(\cos\theta) \begin{matrix}\cos\\ \sin\end{matrix} \phi \\ \psi^{(3)}_{\substack{e\\o}mn} = h_n^{(1)}(kR)\, P_n^m(\cos\theta) \begin{matrix}\cos\\ \sin\end{matrix} \phi, \end{cases}$$

$$\vec{M}_{\substack{e\\o}mn} = \nabla \times (\psi_{\substack{e\\o}mn} \vec{R}),$$

and

$$\vec{N}_{\substack{e\\o}mn} = \frac{1}{k} \nabla \times \nabla \times (\psi_{\substack{e\\o}mn} \vec{R}) .$$

Primed functions are defined with respect to (R', θ', ϕ'):

$$\alpha_n = -j_n(x)/h_n^{(1)}(x)\Big|_{x=ka}$$

and

$$\beta_o = -\frac{\partial}{\partial x}[x j_n(x)] / \frac{\partial}{\partial x}[x h_n^{(1)}(x)]\Big|_{x=ka} .$$

Far-zone Field of a Radially Oriented Dipole on the Surface of a Perfectly Conducting Sphere

The current distribution function for an electric dipole with moment $\vec{p} = p_r \hat{R}$ can be written as

$$(8) \qquad \vec{J}' = -j\omega p_r \hat{R} \, \frac{\delta(R' - \theta)\, \delta(\theta' - \theta_o)\, \delta(\phi' - \phi_o)}{R'^2 \sin\theta'} \, .$$

Substituting Eq. (8) into Eq. (5) one obtains

$$(9) \qquad \vec{E} = \omega^2 \mu p_r \left(\frac{ik}{4\pi}\right) \sum_{n=1}^{\infty} \sum_{m=0}^{n} (2-\delta_o) \, \frac{2n+1}{n(n+1)} \cdot \frac{(n-m)!}{(n+m)!} \iiint \hat{a}_r \, \frac{\delta(R'-a)\, \delta(\theta'-\theta_o)\, \delta(\phi-\phi_o)}{R'^2 \sin\theta'}$$

$$\cdot \left\{ [\vec{M}'^{(1)} + \alpha_n \vec{M}'^{(3)}] \vec{M}^{(3)} + [\vec{N}'^{(1)} + \beta_n \vec{N}'^{(3)}] \vec{N}^{(3)} \right\} dv'$$

$$= -\omega^2 \mu p_r \left(\frac{k}{4\pi}\right) \sum_{n=1}^{\infty} \sum_{m=0}^{n} (2-\delta_o)(2n+1) \, \frac{(n-m)!}{(n+m)!} \, P_n^m(\cos\theta_o) \begin{matrix} \cos \\ \sin \end{matrix} m\phi_o$$

$$\cdot \frac{1}{\rho^2 [\rho h_n^{(1)}]'} \Bigg|_{\rho = ka} \vec{N}^{(3)} \, .$$

By making use of the asymptotic formula for $\vec{N}^{(3)}$, when the value of kR is much larger than unity, we have the expression for the far field:

$$(10) \qquad \vec{E} = -\omega^2 \mu p_r \left(\frac{k}{4\pi}\right) \sum_{n=1}^{\infty} \sum_{m=1}^{n} (2-\delta_o)(2n+1) \, \frac{(n-m)!}{(n+m)!} \, P_n^m(\cos\theta_o) \begin{matrix} \cos \\ \sin \end{matrix} m\phi_o$$

$$\cdot \frac{1}{\rho^2 [\rho h_n^{(1)}]'} \Bigg|_{\rho = ka}$$

$$\cdot (-i)^n \, \frac{e^{ikR}}{kR} \left\{ \frac{d}{d\theta} P_n^m(\cos\theta) \begin{matrix} \cos \\ \sin \end{matrix} m\phi \, \hat{\theta} - \frac{m P_n^m(\cos\theta)}{\sin\theta} \begin{matrix} \sin \\ \cos \end{matrix} m\phi \, \hat{\phi} \right\} .$$

In the special case when the dipole is placed at the top of the sphere with the coordinate (a, 0, 0) Eq. (10) reduces to

$$(11)\quad \vec{E} = -\omega^2\mu\, p_r\left(\frac{k}{4\pi}\right)\sum_{n=1}^{\infty}(2n+1)\,\frac{1}{\rho^2\left[\rho h_n^{(1)}\right]'_{\rho=\rho_a}}(-i)^n\,\frac{d}{d\theta}P_n(\cos\theta)\hat{\theta}$$

$$= \frac{p_r k^2}{4\pi\epsilon\rho_a^2}\cdot\frac{e^{ikR}}{kR}\sum_{n=1}(2n+1)(-i)^n\,\frac{1}{\left[\rho h_n^{(1)}\right]'_{\rho=\rho_a}}\,P_n^1(\cos\theta)\,\hat{\theta},$$

where $\rho_a = ka$.

Far-zone Field of a Small Aperture on the Surface of a Perfectly Conducting Sphere

Insertion of the expression for G_e, defined by Eq. (7), into Eq. (6) results in the integral

$$(12)\quad \vec{E}(\vec{R}) = \frac{ik^2}{4\pi}\iint\sum\sum(2-\delta_o)\,\frac{2n+1}{n(n+1)}\cdot\frac{(n-m)!}{(n+m)!}\,(\vec{E}'\times\hat{n})\cdot\Big\{[\vec{N}'^{(1)} + \alpha_n\vec{N}'^{(3)}]\vec{M}^{(3)}$$

$$+ [\vec{M}'^{(1)} + \beta_n\vec{M}'^{(3)}]\,\vec{N}^{(3)}\Big\}ds'.$$

In evaluating the far field use can be made of the asymptotic formulae for $\vec{M}^{(3)}$ and $\vec{N}^{(3)}$, which are

$$(13)\quad \vec{M}^{(3)}_{\substack{e\\o}mn} = (-i)^{n+1}\,\frac{e^{ikR}}{kR}\left[\mp\frac{m}{\sin\theta}P_n^m(\cos\theta)\begin{matrix}\sin\\\cos\end{matrix}m\phi\,\hat{\theta} - \frac{\partial P_n^m}{\partial\theta}\begin{matrix}\cos\\\sin\end{matrix}m\phi\,\hat{\phi}\right]$$

$$= (-i)^{n+1}\,\frac{e^{ikR}}{kR}\,\vec{m}_{\substack{e\\o}mn}$$

and

$$(14)\quad \vec{N}^{(3)}_{\substack{e\\o}mn} = (-i)^n\,\frac{e^{ikR}}{kR}\left[\frac{\partial P_n^m}{\partial\theta}\begin{matrix}\cos\\\sin\end{matrix}m\phi\,\hat{\theta} \mp \frac{m}{\sin\theta}P_n^m(\cos\theta)\begin{matrix}\sin\\\cos\end{matrix}m\phi\,\hat{\phi}\right]$$

$$= (-i)^n\,\frac{e^{ikR}}{kR}\,\vec{n}_{\substack{e\\o}mn},$$

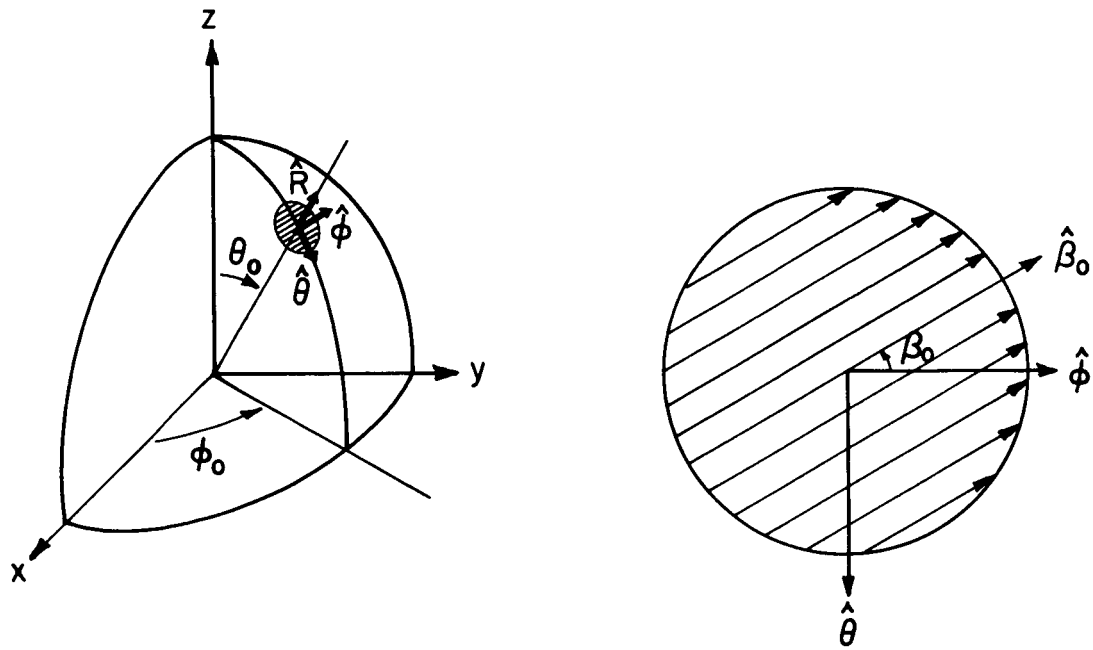

Fig. 2.

where $\hat{R} \times \vec{m} = \vec{n}$. For an infinitesimal aperture with field direction shown in Fig. 2 the aperture field is described by

$$\vec{E}(\vec{R}') = A E_o \hat{\beta}_o \frac{\delta(\theta'-\theta_o)\,\delta(\phi'-\phi_o)}{a^2 \sin\theta} \quad .$$

Equation (12) then becomes

$$(15)\quad \vec{E}(\vec{R}) = \frac{-iAE_o}{4\pi a} \frac{e^{ikR}}{kR} \sum_{n=1}^{\infty} \sum_{m=0}^{n} (-i)^n (2-\delta_o) \frac{2n+1}{n(n+1)} \frac{(n-m)!}{(n+m)!}$$

$$\left\{ \frac{\vec{m}_{e_{omn}}}{\xi_n(ka)} \left[\cos\beta_o \left. \frac{dP_n^m(\cos\theta')}{d\theta'} \right|_{\theta'=\theta_o} \begin{matrix} \cos \\ \sin \end{matrix} m\phi_o \right.\right.$$

$$\left. \mp \sin\beta_o \frac{mP_n^m(\cos\theta_o)}{\sin\theta_o} \begin{matrix} \sin \\ \cos \end{matrix} m\phi_o \right]$$

$$+ \frac{i(\hat{R} \times \vec{m}_{e_{omn}})}{[\xi_n(ka)]'} \left[\mp \cos\beta_o \frac{mP_n^m(\cos\theta_o)}{\sin\theta_o} \begin{matrix} \sin \\ \cos \end{matrix} m\phi_o \right.$$

$$\left.\left. + \sin\beta_o \left. \frac{dP_n^m(\cos\theta')}{d\theta'} \right|_{\theta'=\theta_o} \begin{matrix} \cos \\ \sin \end{matrix} m\phi_o \right] \right\}$$

$$= - \frac{iAE_o}{4\pi a} \frac{e^{ikR}}{R} \sum_{n=1}^{\infty} \sum_{m=0}^{n} (-i)^n (2-\delta_o) \frac{2n+1}{n(n+1)} \frac{(n-m)!}{(n+m)!} [F_\theta \hat{\theta} + F_\phi \hat{\phi}],$$

where

$$F_\theta = \frac{1}{\xi_n(ka)} \frac{m P_n^m(\cos\theta)}{\sin\theta} \left[-\cos\beta_o \sin m(\phi-\phi_o) \frac{dP_n^m(\cos\theta')}{d\theta'} \Big|_{\theta'=\theta_o} \right.$$

$$\left. + \sin\beta_o \cos m(\phi-\phi_o) \frac{m P_n^m(\cos\theta_o)}{\sin\theta_o} \right]$$

$$+ \frac{i}{[\xi_n(ka)]'} \frac{dP_n^m(\cos\theta)}{d\theta} \left[-\cos\beta_o \sin m(\phi-\phi_o) \frac{m P_n^m(\cos\theta_o)}{\sin\theta_o} \right.$$

$$\left. + \sin\beta_o \cos m(\phi-\phi_o) \frac{dP_n^m(\cos\theta')}{d\theta'} \Big|_{\theta'=\theta_o} \right],$$

$$F_\phi = \frac{1}{\xi_n(ka)} \frac{dP_n^m(\cos\theta)}{d\theta} \left[-\cos\beta_o \cos m(\phi-\phi_o) \frac{dP_n^m(\cos\theta')}{d\theta'} \Big|_{\theta'=\theta_o} \right.$$

$$\left. - \sin\beta_o \sin m(\phi-\phi_o) \frac{m P_n^m(\cos\theta_o)}{\sin\theta_o} \right]$$

$$+ \frac{i}{[\xi_n(ka)]'} \frac{m P_n^m(\cos\theta)}{\sin\theta} \left[-\cos\beta_o \cos m(\phi-\phi_o) \frac{m P_n^m(\cos\theta_o)}{\sin\theta_o} \right.$$

$$\left. - \sin\beta_o \sin m(\phi-\phi_o) \frac{dP_n^m(\cos\theta')}{d\theta'} \Big|_{\theta'=\theta_o} \right],$$

$$\xi_n = \xi_n(ka) = ka\, h_n^{(1)}(ka),$$

and

$$\xi_n' = [\xi_n(ka)]' = \frac{d}{dx} [\xi_n(x)]_{x=ka} = h^{(1)}(ka) + ka \frac{d}{dx} h_n^{(1)} \Big|_{x=ka}.$$

In the special case when the aperture is on the top of the sphere with coordinate (a, 0, 0), Eq. (15) reduces to

$$(16)\quad \vec{E}(\vec{R}) = -\frac{AE}{4\pi a}\,\frac{e^{ikR}}{R}\sum_{n=1}^{\infty}(-i)^n\,\frac{2n+1}{n(n+1)}\left\{[\cos\beta_o\sin\phi-\sin\beta_o\cos\phi]\cdot\left[\frac{-i}{\xi_n}\,\frac{P_n'(\cos\theta)}{\sin\theta}+\frac{dP_n'(\cos\theta)}{d\theta}\,\frac{1}{\xi_n'}\right]\hat{\theta}\right.$$

$$\left.+[\cos\beta_o\cos\phi+\sin\beta_o\sin\phi]\left[\frac{-i}{\xi_n}\,\frac{dP_n'(\cos\theta)}{d\theta}+\frac{1}{\xi_n'}\,\frac{P_n'(\cos\theta)}{\sin\theta}\right]\hat{\phi}\right\}.$$

Transformation of Coordinates

In programming Eqs. (10) and (15) for a digital computer, difficulties will be encountered in determining the number of terms needed in the series since double summation over index m and n is required. In contrast, only a single summation is necessary for Eqs. (11) and (16) and it is much easier to handle.

The troublesome problem for programming Eqs. (10) and (15) for calculating the far-field pattern of an arbitrarily located dipole or aperture can be avoided by a method which is described in the following paragraphs.

For an arbitrarily located dipole (or aperture) with coordinate (a, θ_o, ϕ_o) on the sphere, the coordinate system is first rotated around the z-axis through the angle ϕ_o, and then followed by tilting the rotated coordinate system an angle of θ_o so that the coordinate of the dipole (or aperture) in the new coordinate system will be (a, 0, 0). It is in this new coordinate system that the simplified formulae shown in Eq. (11) (or Eq. (16)) can be used. For each direction specified by θ and ϕ in the original coordinate system the corresponding coordinates θ' and ϕ' in the new coordinate system will be

$$(17)\quad \theta' = \cos^{-1}[\cos\theta_o\cos\theta+\sin\theta_o\sin\theta\cos(\phi-\phi_o)]$$

and

$$(18)\quad \phi' = \cot^{-1}\frac{\cos\theta_o\sin\theta\cos(\phi-\phi_o)-\sin\theta_o\cos\theta}{\sin\theta\sin(\phi-\phi_o)}\,.$$

The transformation of the unit vectors can be obtained by taking the gradients of $\cos\theta'$ and $\cot\phi'$ in the two coordinate systems

$$(19)\qquad \nabla\cos\theta' = \frac{\underline{e}_{\theta'}}{R}\,\frac{\partial}{d\theta'}[\cos\theta'] = -\frac{\underline{e}_{\theta'}}{R}\sin\theta' ,$$

$$(20)\qquad \nabla\cos\theta' = \nabla[\cos\theta_o\cos\theta + \sin\theta_o\sin\theta\cos(\phi-\phi_o)]$$

$$= \frac{\underline{e}_\theta}{R}[-\cos\theta_o\sin\theta + \sin\theta_o\sin\theta\cos(\phi-\phi_o)]$$

$$+\frac{\underline{e}_\phi}{R\sin\theta}[-\sin\theta_o\sin\theta\sin(\phi-\phi_o)],$$

$$(21)\qquad \nabla\cot\phi' = \frac{\underline{e}_{\phi'}}{R\sin\theta'}\left[\frac{\partial}{\partial\phi'}(\cot\phi')\right] = -\frac{\underline{e}_{\phi'}}{R\sin\theta'}\csc^2\phi',$$

and

$$(22)\qquad \nabla\cot\phi' = \nabla\left[\frac{\cos\theta_o\sin\theta\cos(\phi-\phi_o)-\sin\theta_o\cos\theta}{\sin\theta\sin(\phi-\phi_o)}\right]$$

$$= \nabla\left[\cos\theta_o\cot(\phi-\phi_o) - \frac{\sin\theta_o\cot\theta}{\sin(\phi-\phi_o)}\right]$$

$$= \frac{\underline{e}_\theta}{R}\left[\frac{\sin\theta_o}{\sin(\phi-\phi_o)}\csc^2\theta\right] + \frac{\underline{e}_\phi}{R\sin\theta}$$

$$\cdot\left\{\csc^2(\phi-\phi_o)[\sin\theta_o\cot\theta\cos(\phi-\phi_o)-\cos\theta_o]\right\}.$$

Equating the gradients of the same functions in the two coordinate systems given by Eqs. (19), (20), (21), and (22) the following relations are obtained for the unit vectors:

$$(23)\qquad \underline{e}_{\theta'}\sin\theta' = \underline{e}_\theta[\cos\theta_o\sin\theta - \sin\theta_o\cos\theta\cos(\phi-\phi_o)]$$

$$+\underline{e}_\phi\sin\theta_o\sin(\phi-\phi_o)$$

and

$$(24)\quad \frac{\underline{e}_{\phi'}}{\sin\theta' \sin^2\phi'} = -\underline{e}_{\theta}\left[\frac{\sin\theta_o}{\sin^2\theta \sin(\phi-\phi_o)}\right] - \frac{\underline{e}_{\phi}}{\sin\theta}\left[\frac{\sin\theta_o \cot\theta \cos(\phi-\phi_o)-\cos\theta_o}{\sin^2(\phi-\phi_o)}\right].$$

The far field of an arbitrarily located dipole (or aperture) is then evaluated first in the rotated coordinate system by Eq. (11) (or Eq. (16)) with the appropriate angular coordinates given by Eqs. (17) and (18). The field components thus acquired are converted back to the original coordinate system through the use of Eqs. (23) and (24). If several sources (dipoles or apertures) are assumed, the procedures described above must be repeated and the sum of those field components gives the resultant field.

Numerical Computation

Equations (11), (16), (18), (23), and (24) are programmed for the computer IBM 7094. A subroutine has been used for generating spherical Bessel and Neumann functions for real arguments and positive integral orders described by Corbato and Uretsky.[3] Twenty-five terms are summed in those series. To assume convergence and to confine the errors within one per cent in the summation of the series, the diameter of the sphere is limited to a value of less than four wavelengths. The results are normalized for each group with the same configuration of sources and the same diameter of the sphere. Patterns are shown in Figs. 3-10 for the dipole source case and Figs. 11-16 for the aperture source case. The four sources on the sphere are symmetrically located with coordinate $\theta = 0°$, $\phi = 0°$; $\theta = 109.5°$, $\phi = 0°$; $\theta = 109.5°$, $\phi = 120°$; and $\theta = 109.5°$, $\phi = 240°$, respectively.

In summing those series the summation was stopped when the ratio of the absolute value of the sum of the last four terms and the absolute value of the total sum is less than 10^{-5}. This criterion limits the argument in the spherical Bessel and Neumann functions to less than 12 (corresponding to a diameter of the sphere less than 4λ) in order to terminate the summation within 25 terms. The subroutine for the spherical Bessel and Neumann functions can still be used for orders higher than 25 and larger arguments, but the routine used for the Legendre will give more cumulated errors for higher order terms. In addition, there are errors caused by transformation of coordinates and unit vectors which are not easy to estimate. Fewer errors are involved when the sources are dipoles because only Eqs. (17) and (23) were used (use must be made of Eqs. (18) and (24) also for aperture excitation) since there is no ϕ field component.

The corresponding diameter of the sphere, the angle ϕ, and the field direction angle β on the aperture (for the aperture source case only) are indicated in each pattern. The right half of the pattern assumes the smaller value of the two ϕ's indicated. The angle β is the same for all four apertures on the sphere, i.e., it is either 0° or 90°.

The results are normalized for each group (all patterns in the same figure) with respect to the largest data value obtained in that group. The largest data value may not necessarily be the actual maximum value since the position of the maximum of the radiation pattern may not be in the planes which have been chosen.

In the dipole source case the fields are evaluated between angles $\phi = 0°$ and $\phi = 60°$ with the incremental angle $\Delta\phi = 10°$. Because of the symmetrical situation the field from $\phi = 0°$ to $\phi = 60°$ covers all its variations. In the aperture source case, with $\beta = 0°$, patterns in the plane $\phi = 0°$ and 180°, $\phi = 45°$ and 225°, $\phi = 90°$ and 270°, and $\phi = 135°$ and 315° are presented. For the case in which $\beta = 90°$, patterns in the plane $\phi = 0°$ and 180°, $\phi = 45°$ and 225°, and $\phi = 90°$ and 270° are presented. By symmetry, the patterns in the plane $\phi = 135°$ and 315° are the same as those in the plane $\phi = 45°$ and 225°, except that the right half and the left half of the pattern are interchanged.

In several planes which have been chosen to show patterns, there are either no E_θ or no E_ϕ components. For example, Fig. 3 shows no E_ϕ component in the plane $\phi = 0°$ and 180°, and in Fig. 11 there is no E_θ component in the plane $\phi = 0°$ and 180°, etc.

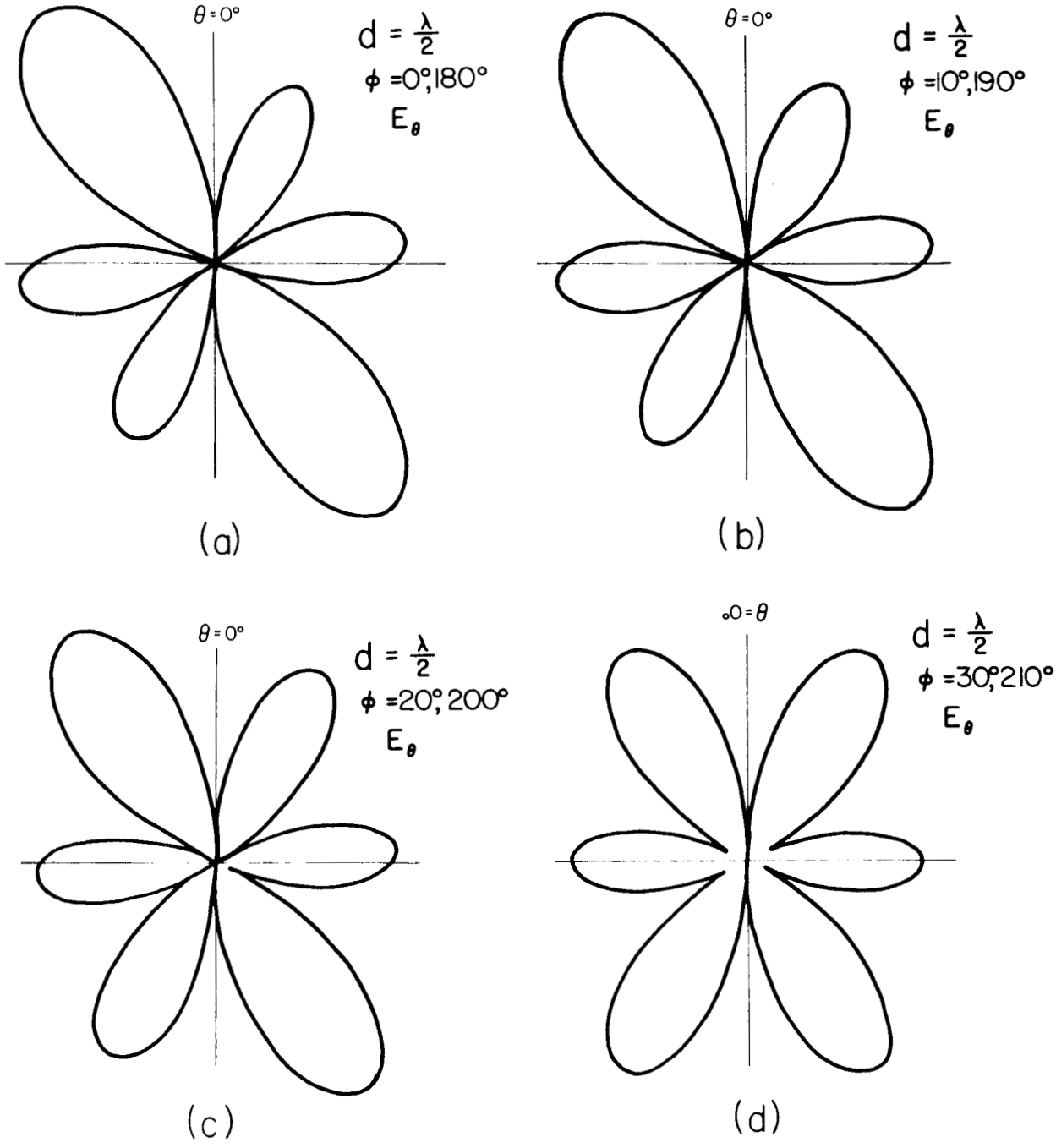

Fig. 3. Radiation patterns of four dipoles, symmetrically located and radially oriented on the surface of a sphere of diameter equal to $\lambda/2$.

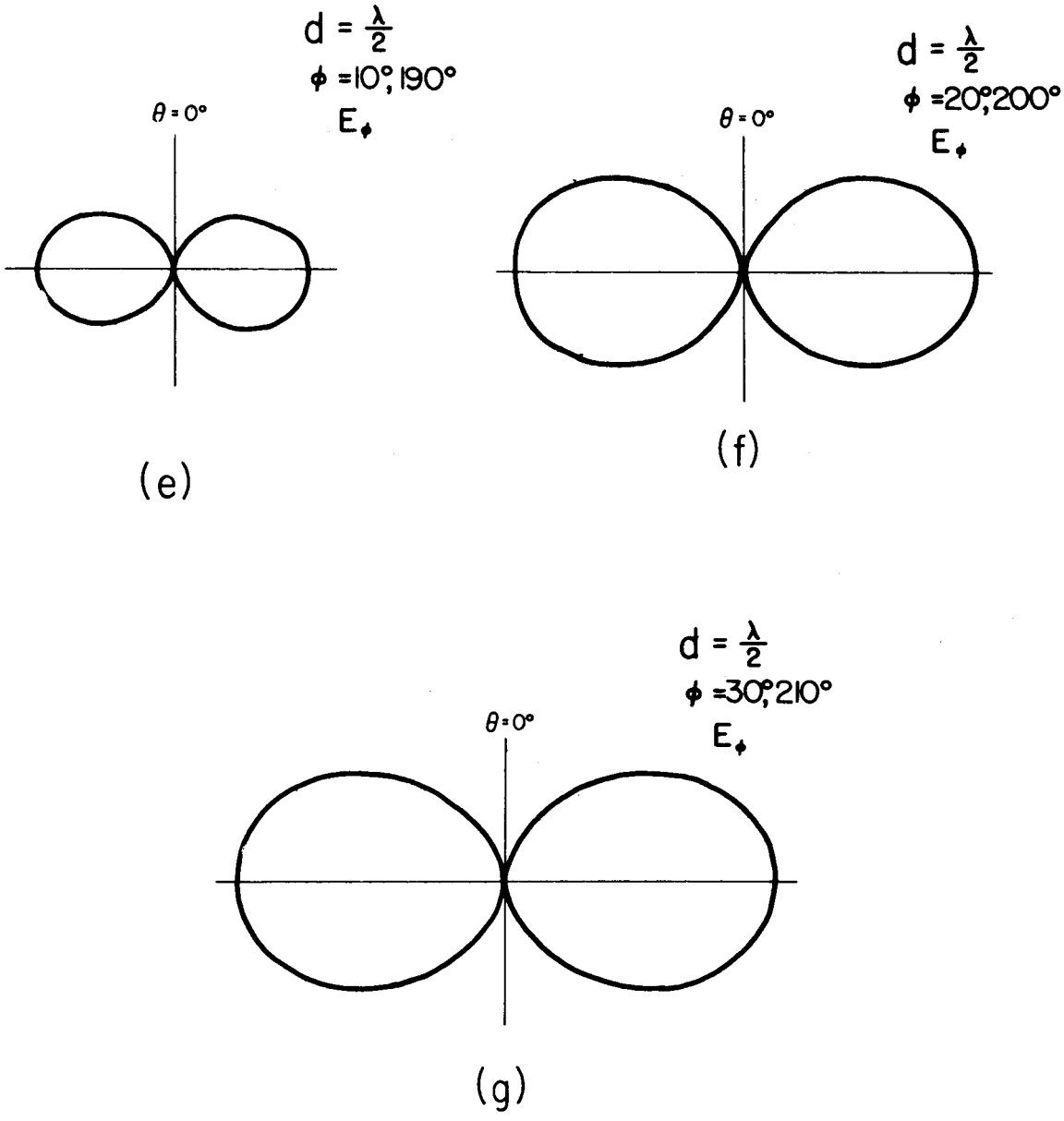

Fig. 3. Radiation patterns of four dipoles, symmetrically located and radially oriented on the surface of a sphere of diameter equal to $\lambda/2$.

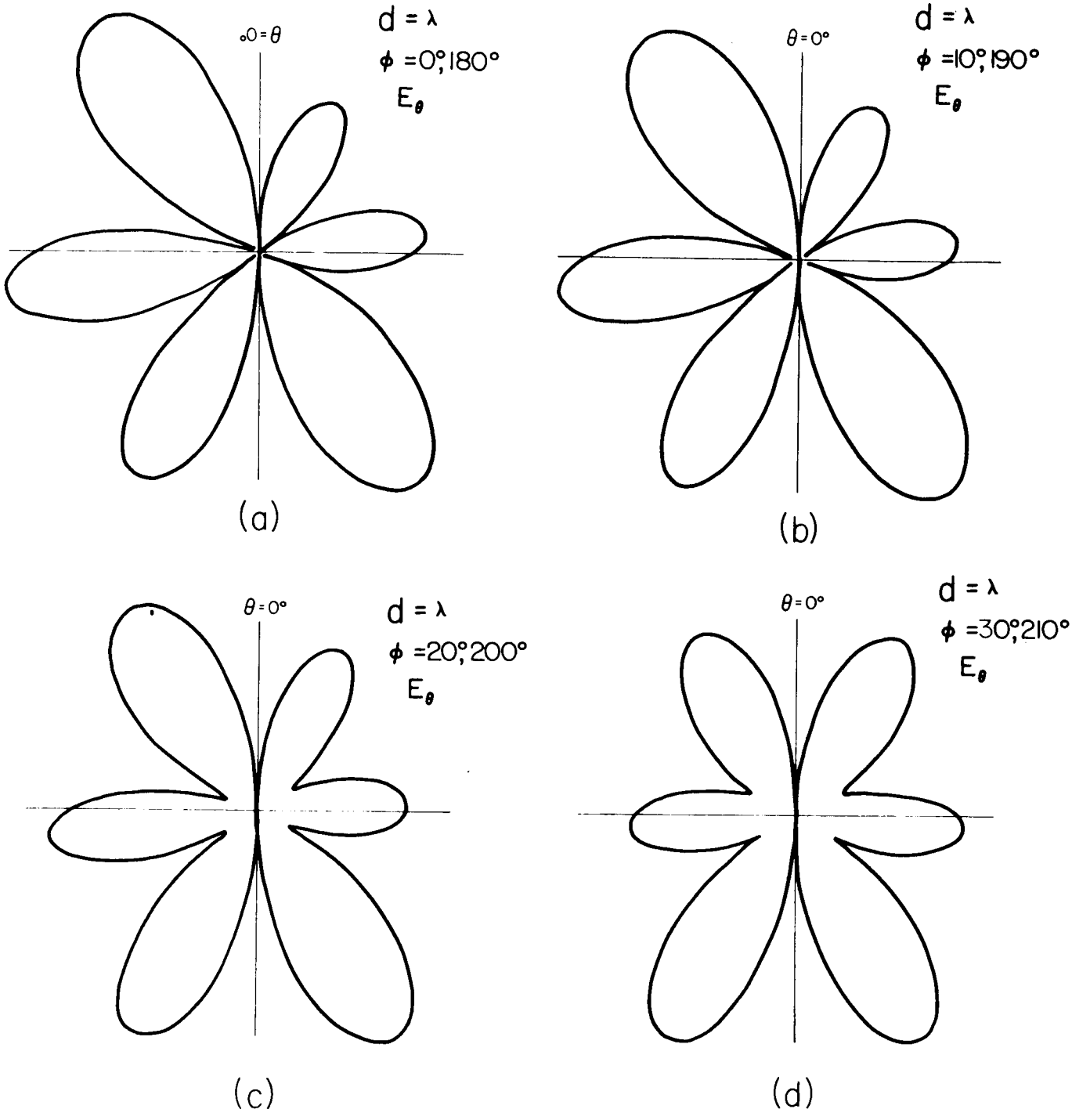

Fig. 4. Radiation patterns of four dipoles, symmetrically located and radially oriented on the surface of a sphere of diameter equal to λ.

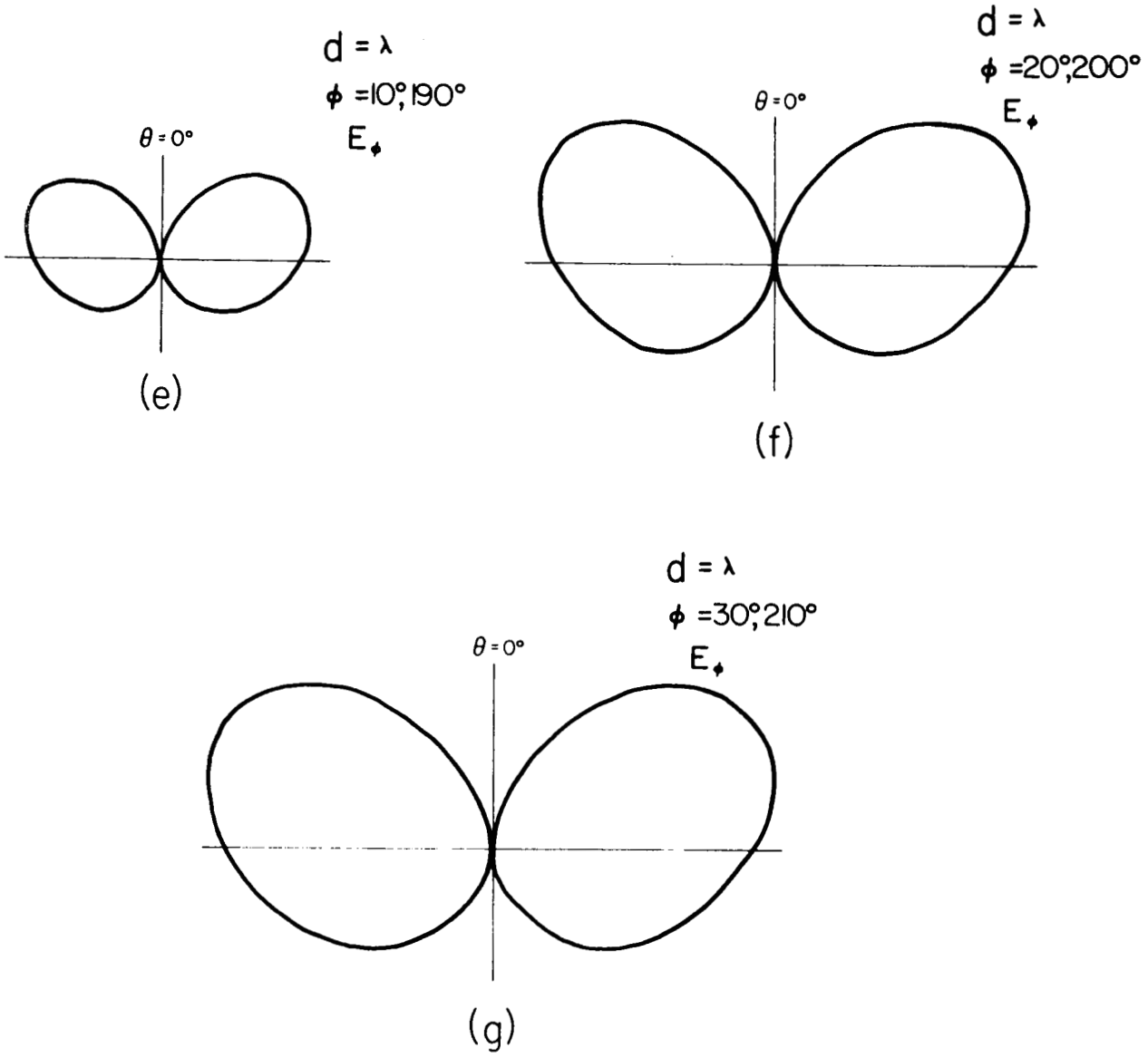

Fig. 4. Radiation patterns of four dipoles, symmetrically located and radially oriented on the surface of a sphere of diameter equal to λ.

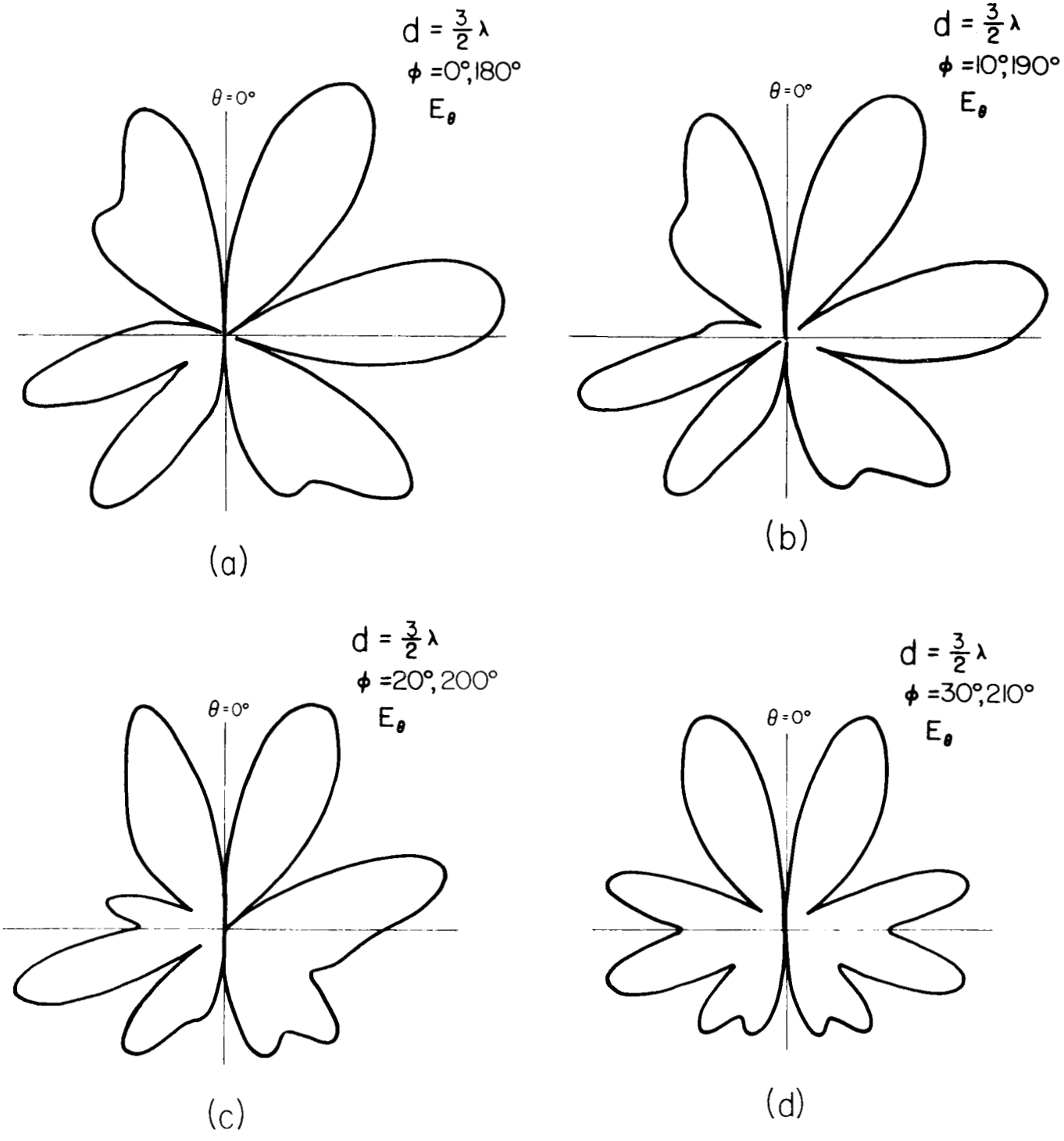

Fig. 5. Radiation patterns of four dipoles, symmetrically located and radially oriented on the surface of a sphere of diameter equal to $3\lambda/2$.

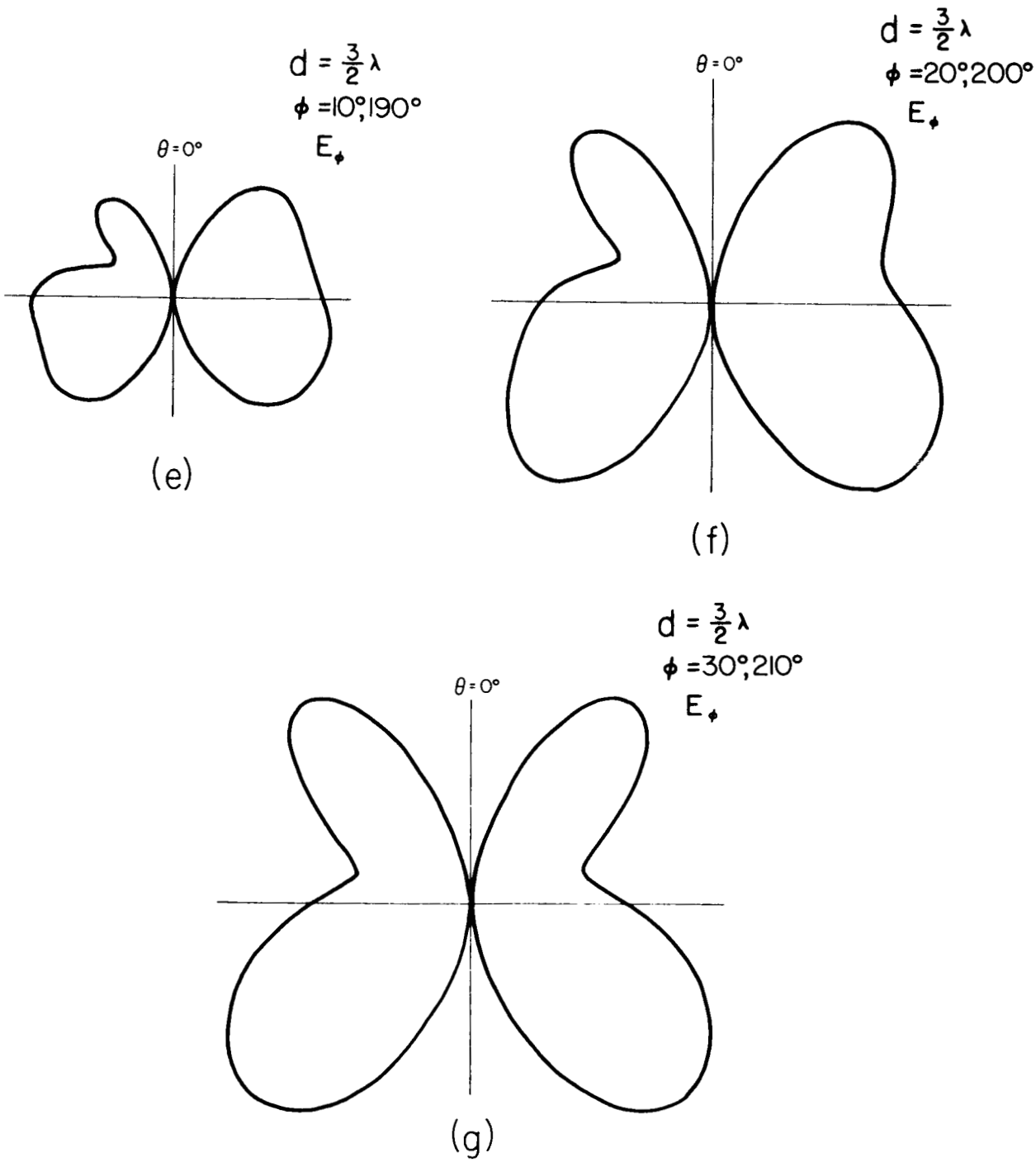

Fig. 5. Radiation patterns of four dipoles, symmetrically located and radially oriented on the surface of a sphere of diameter equal to $3\lambda/2$.

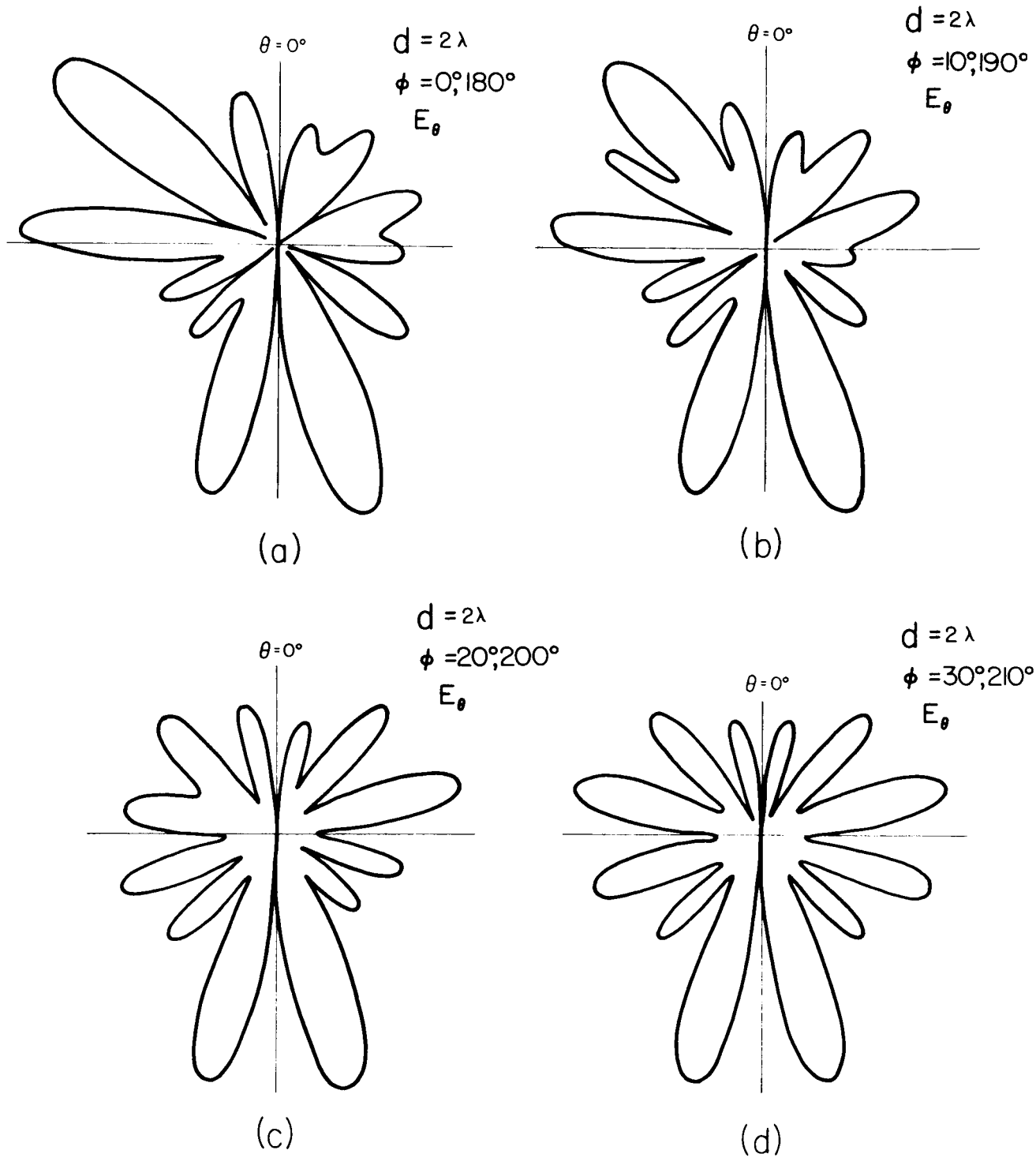

Fig. 6. Radiation patterns of four dipoles, symmetrically located and radially oriented on the surface of a sphere of diameter equal to 2λ.

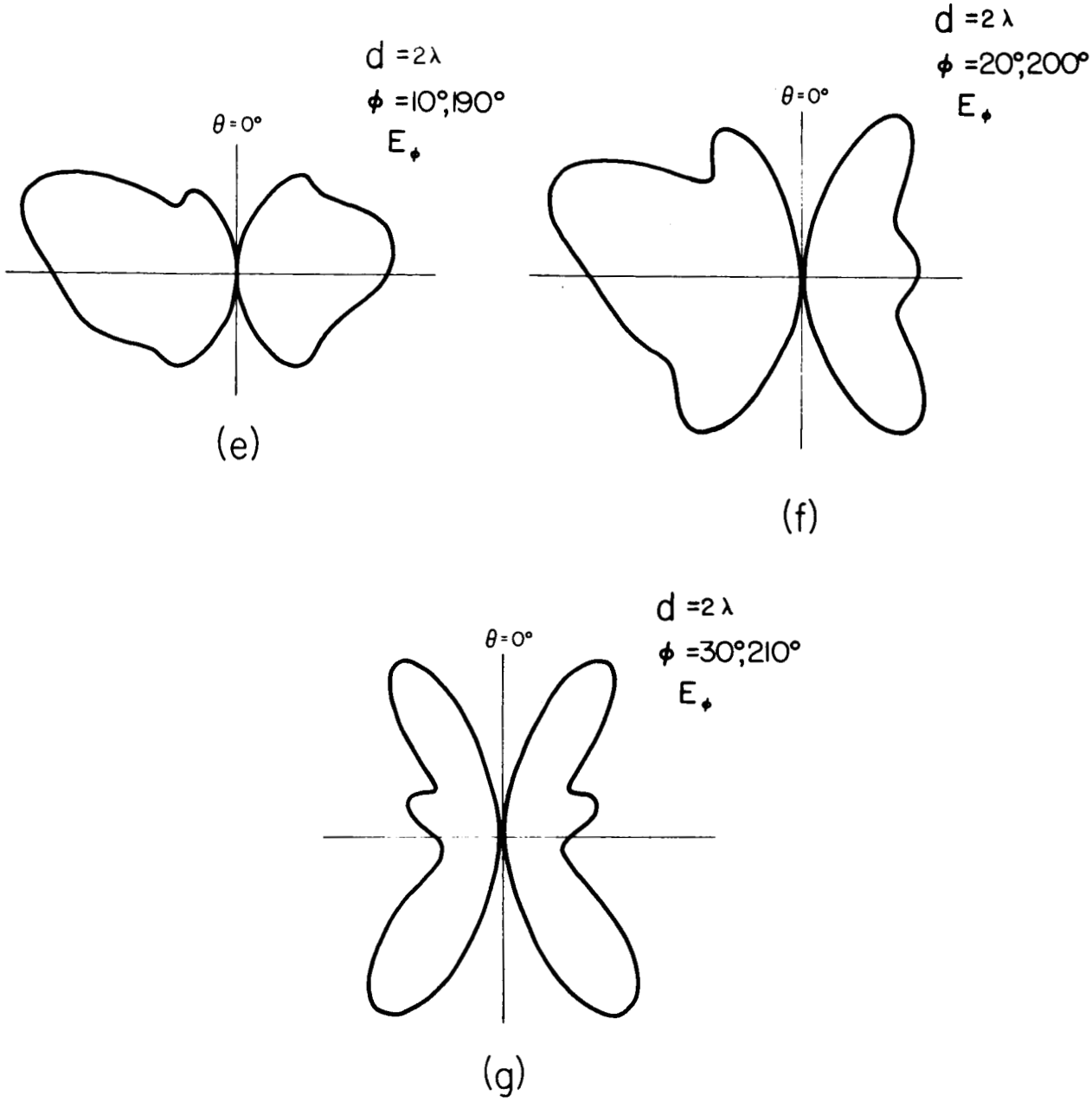

Fig. 6. Radiation patterns of four dipoles, symmetrically located and radially oriented on the surface of a sphere of diameter equal to 2λ.

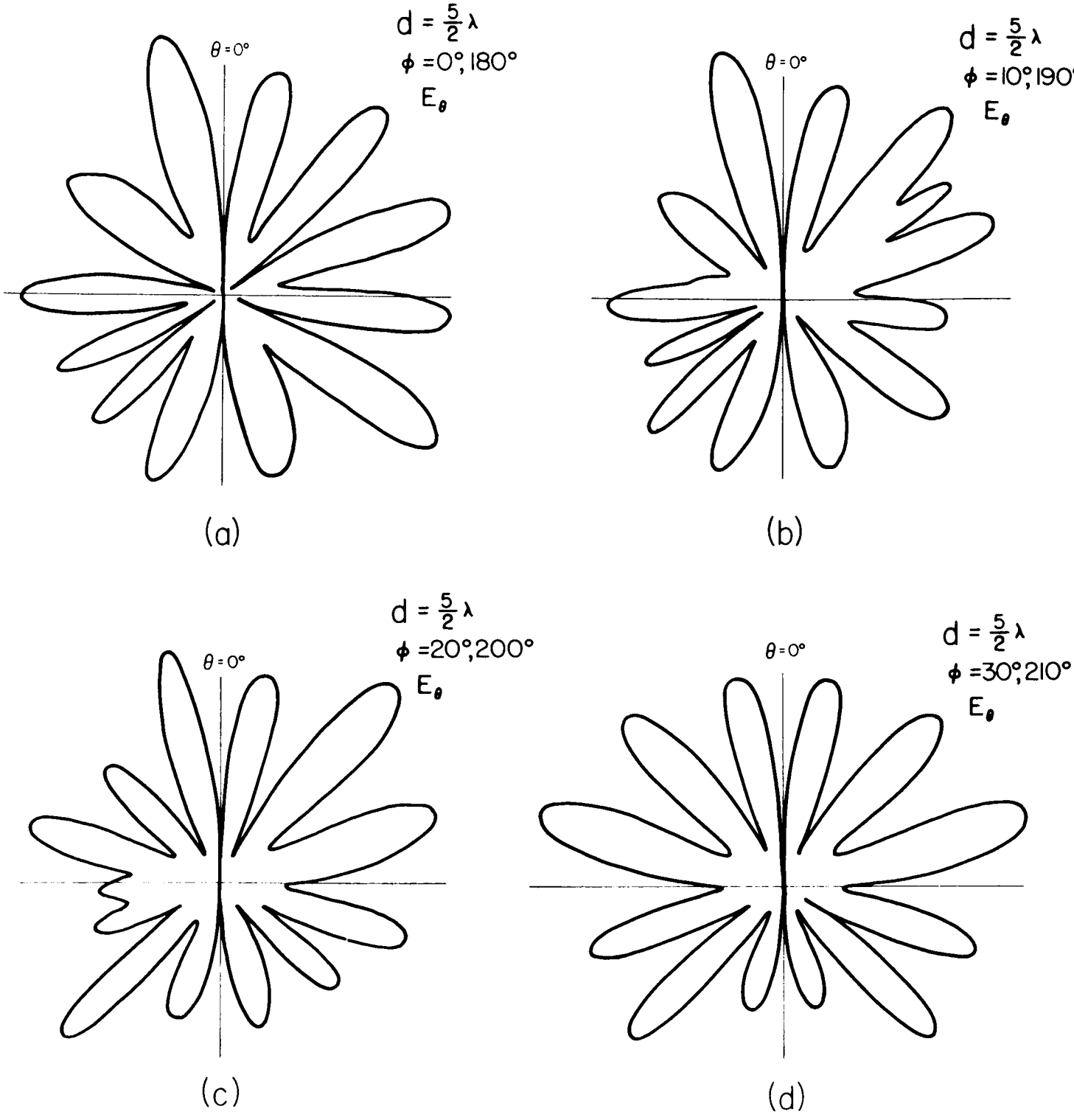

Fig. 7. Radiation patterns of four dipoles, symmetrically located and radially oriented on the surface of a sphere of diameter equal to $5\lambda/2$.

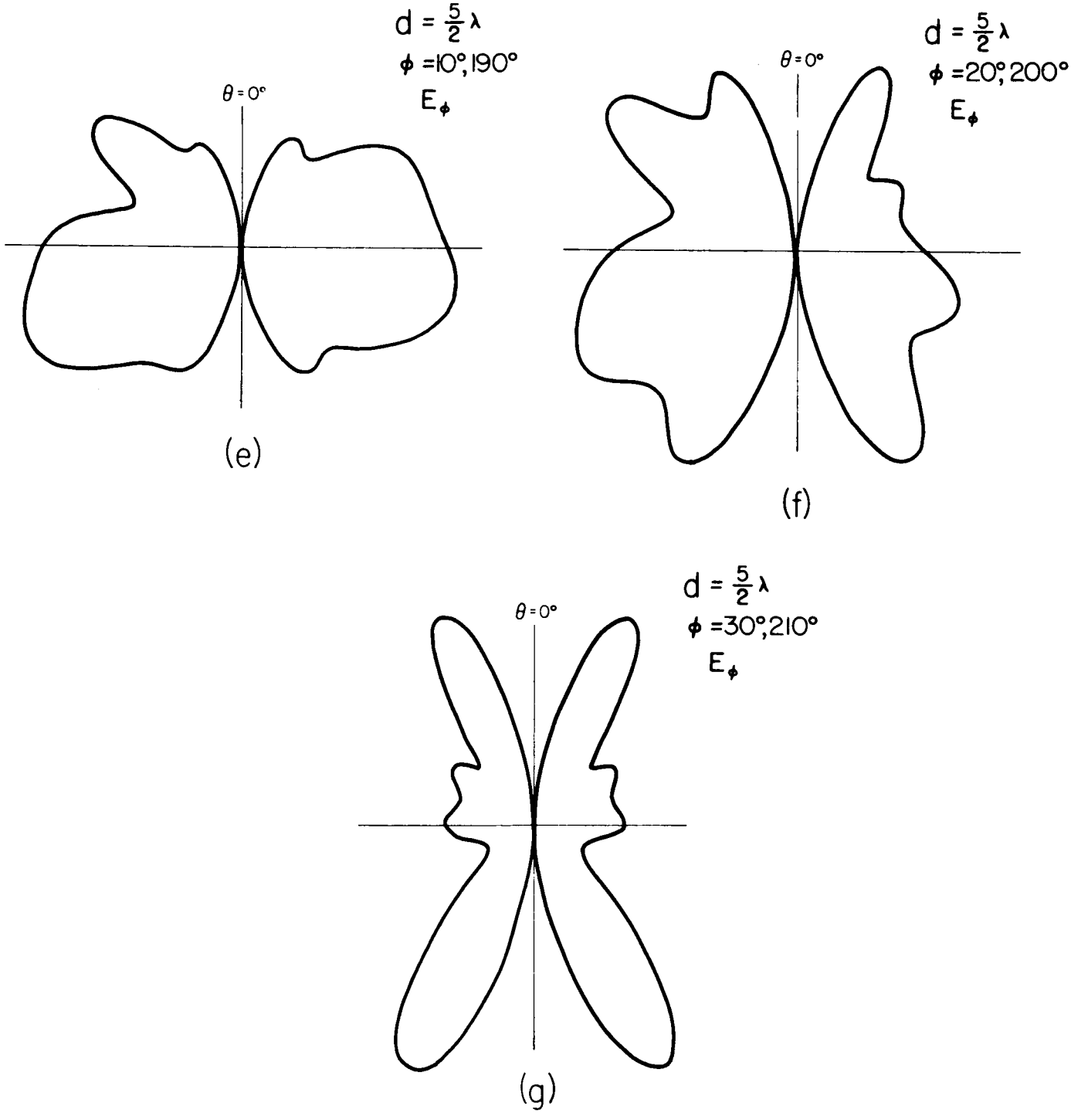

Fig. 7. Radiation patterns of four dipoles, symmetrically located and radially oriented on the surface of a sphere of diameter equal to $5\lambda/2$.

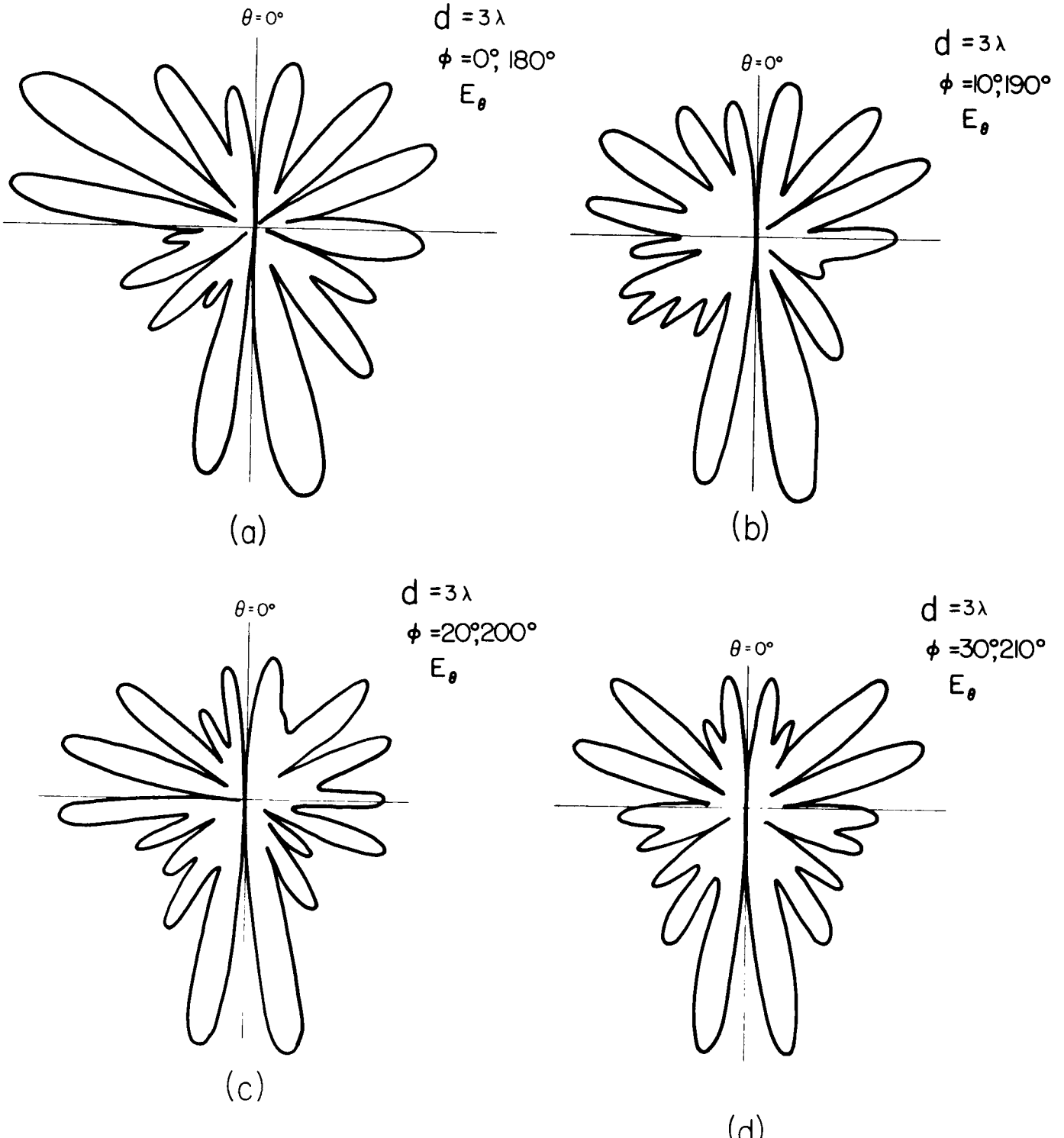

Fig. 8. Radiation patterns of four dipoles, symmetrically located and radially oriented on the surface of a sphere of diameter equal to 3λ.

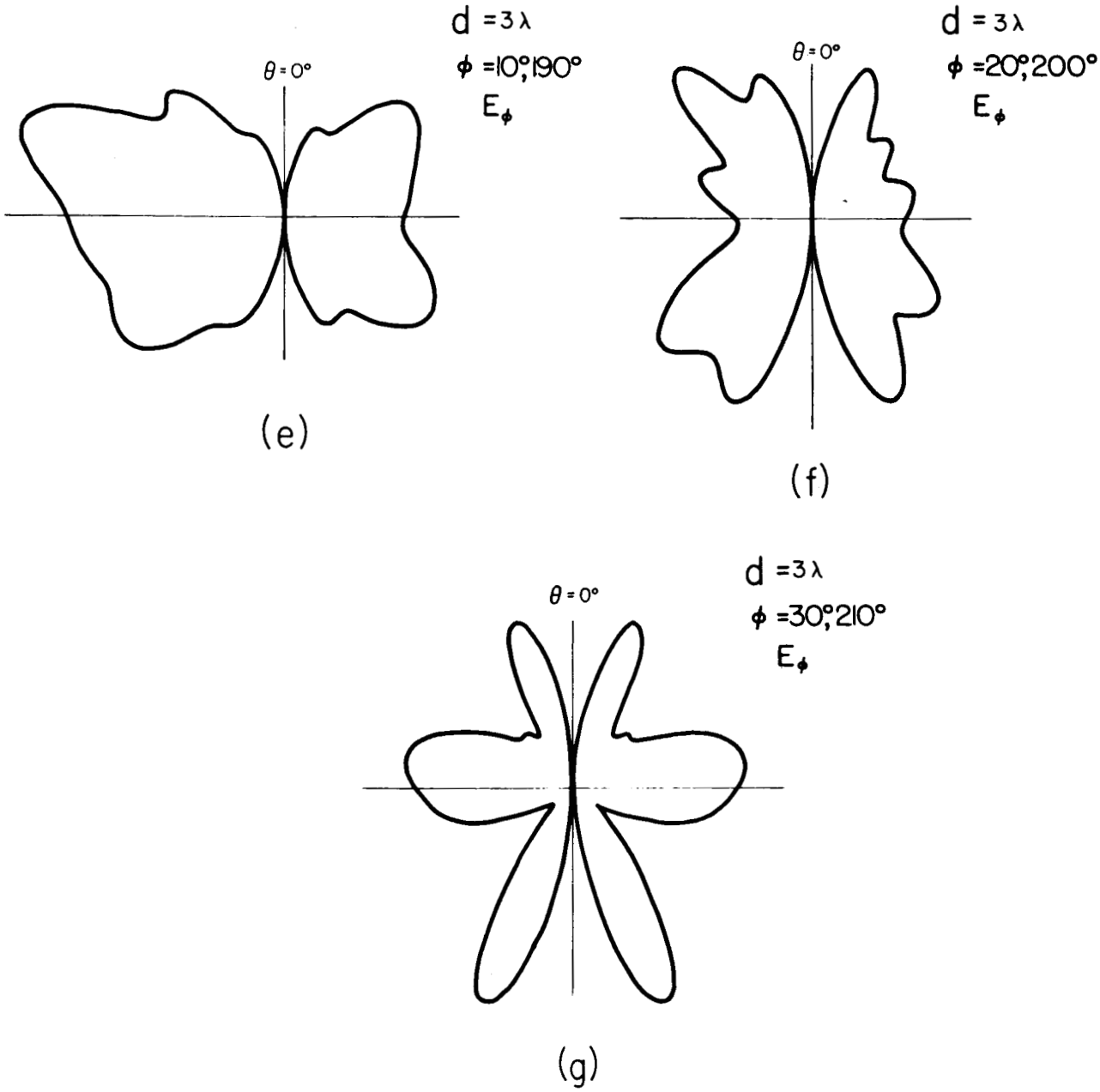

Fig. 8. Radiation patterns of four dipoles, symmetrically located and radially oriented on the surface of a sphere of diameter equal to 3λ.

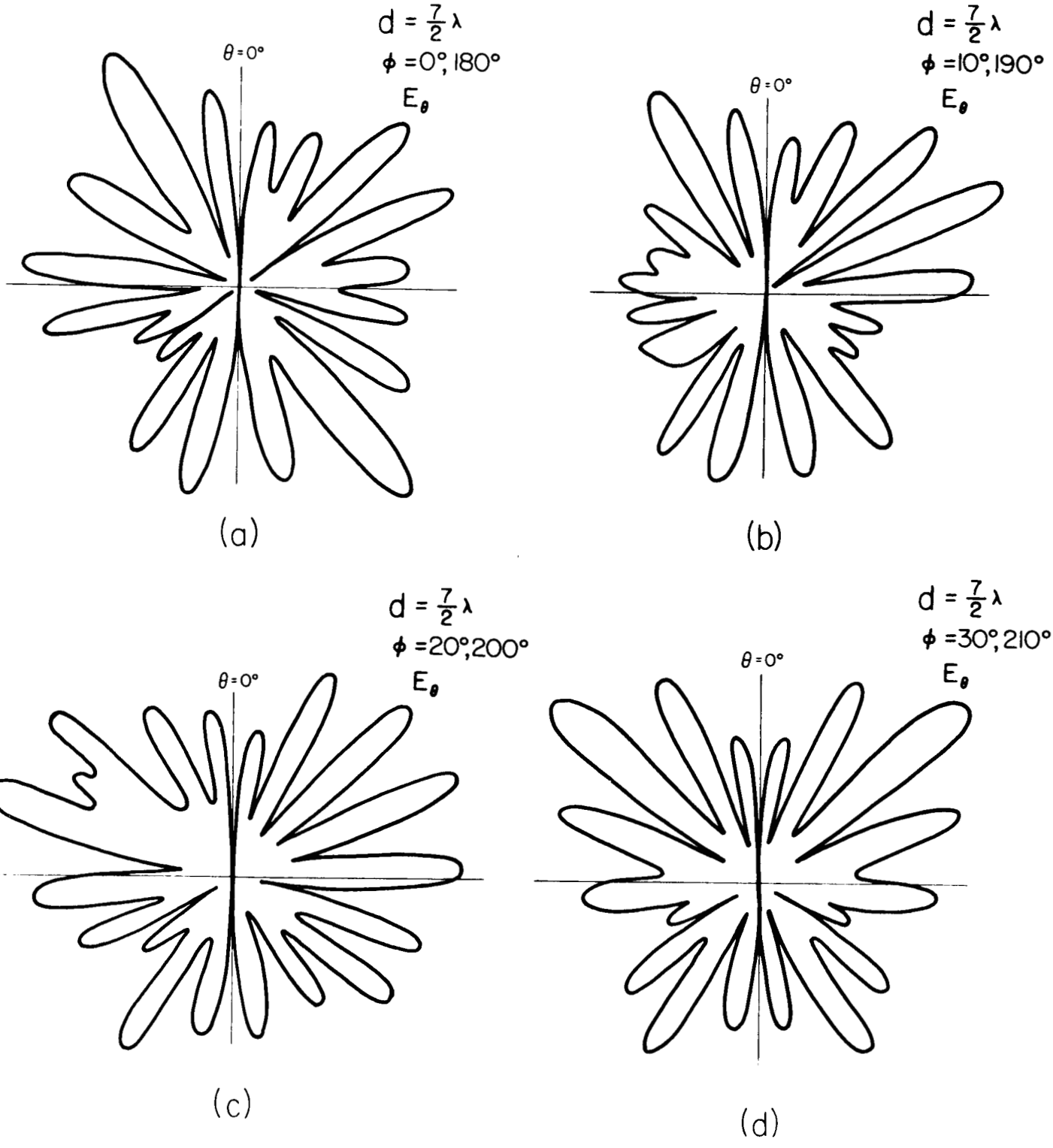

Fig. 9. Radiation patterns of four dipoles, symmetrically located and radially oriented on the surface of a sphere of diameter equal to $7\lambda/2$.

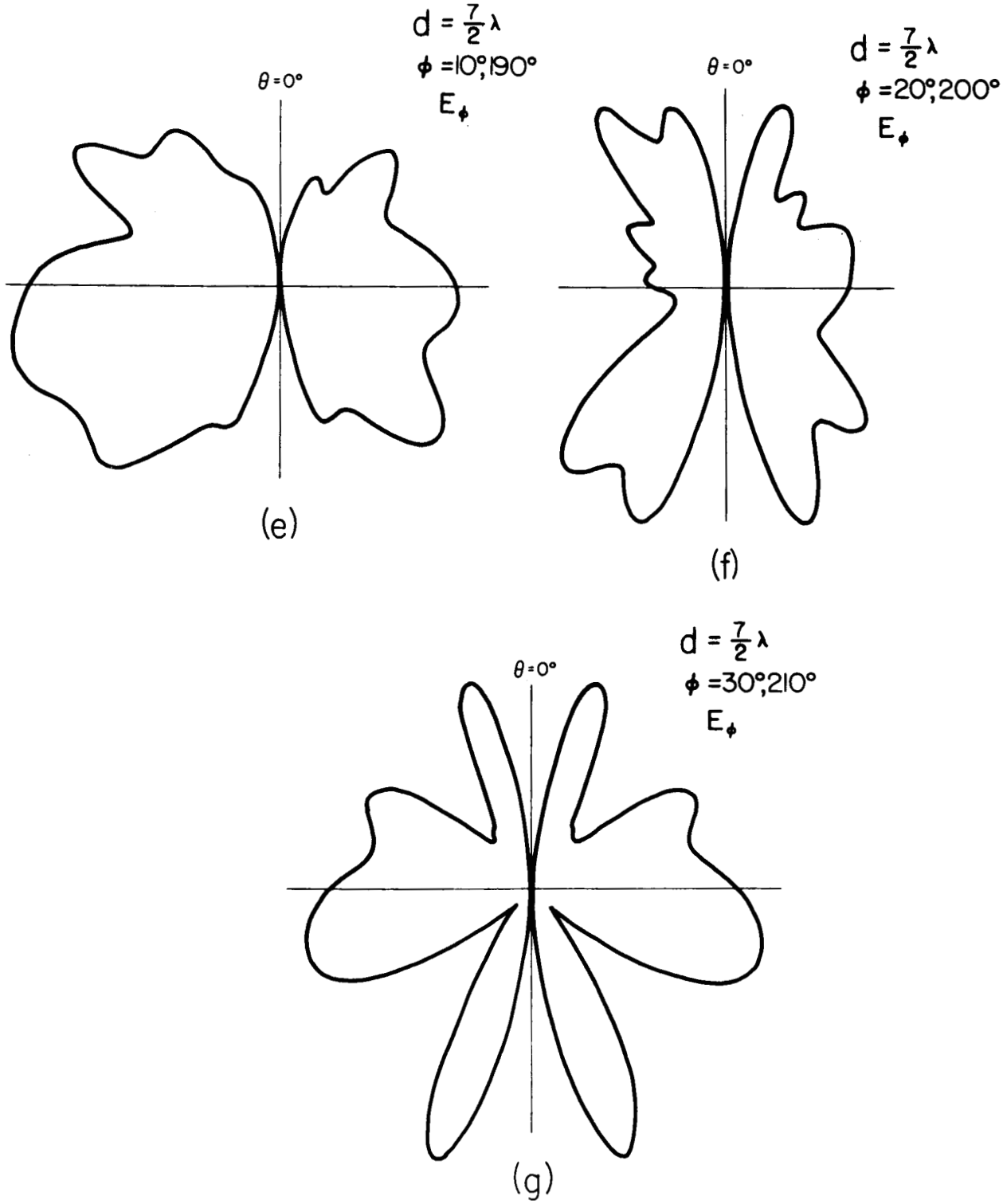

Fig. 9. Radiation patterns of four dipoles, symmetrically located and radially oriented on the surface of a sphere of diameter equal to $7\lambda/2$.

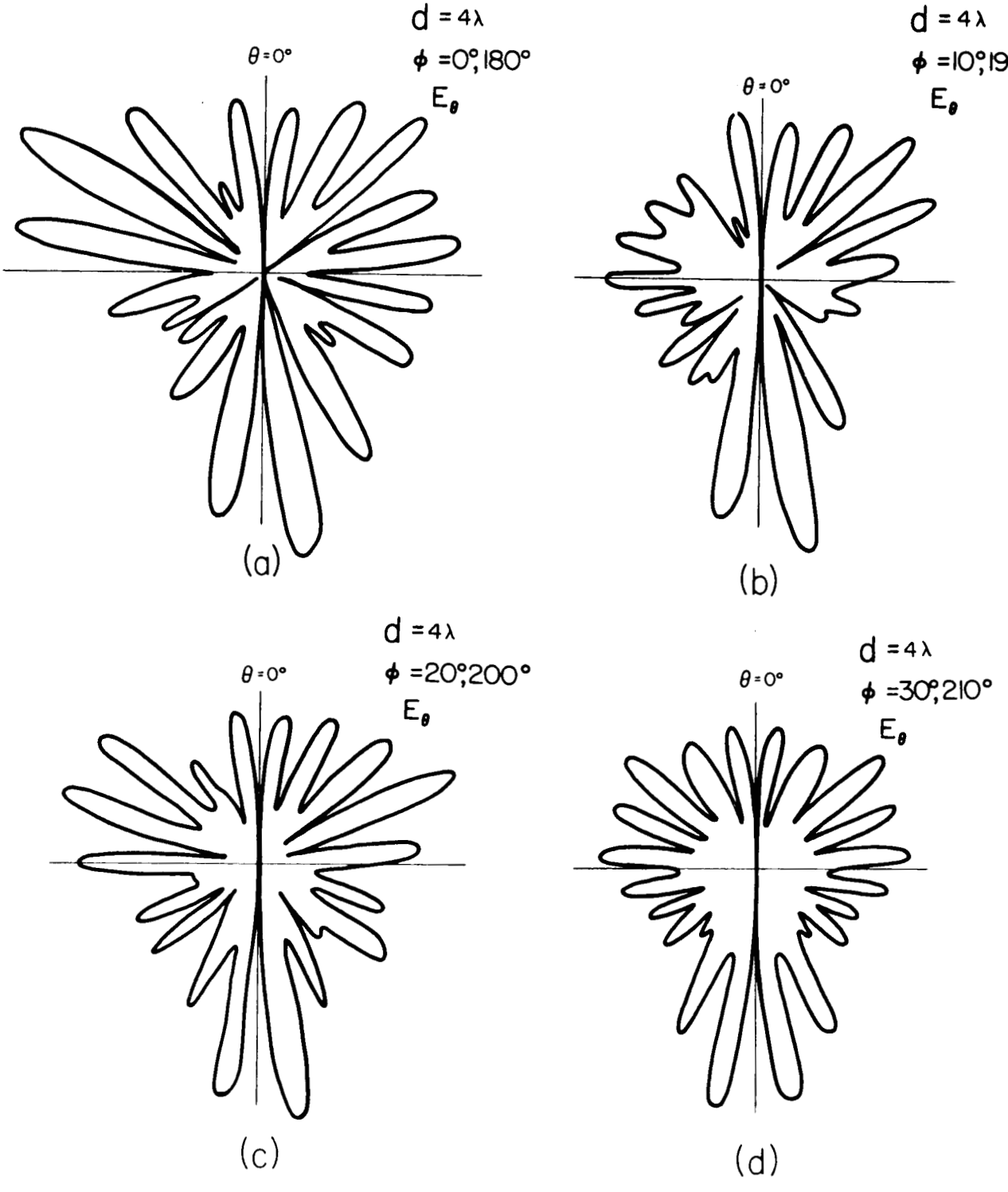

Fig. 10. Radiation patterns of four dipoles, symmetrically located and radially oriented on the surface of a sphere of diameter equal to 4λ .

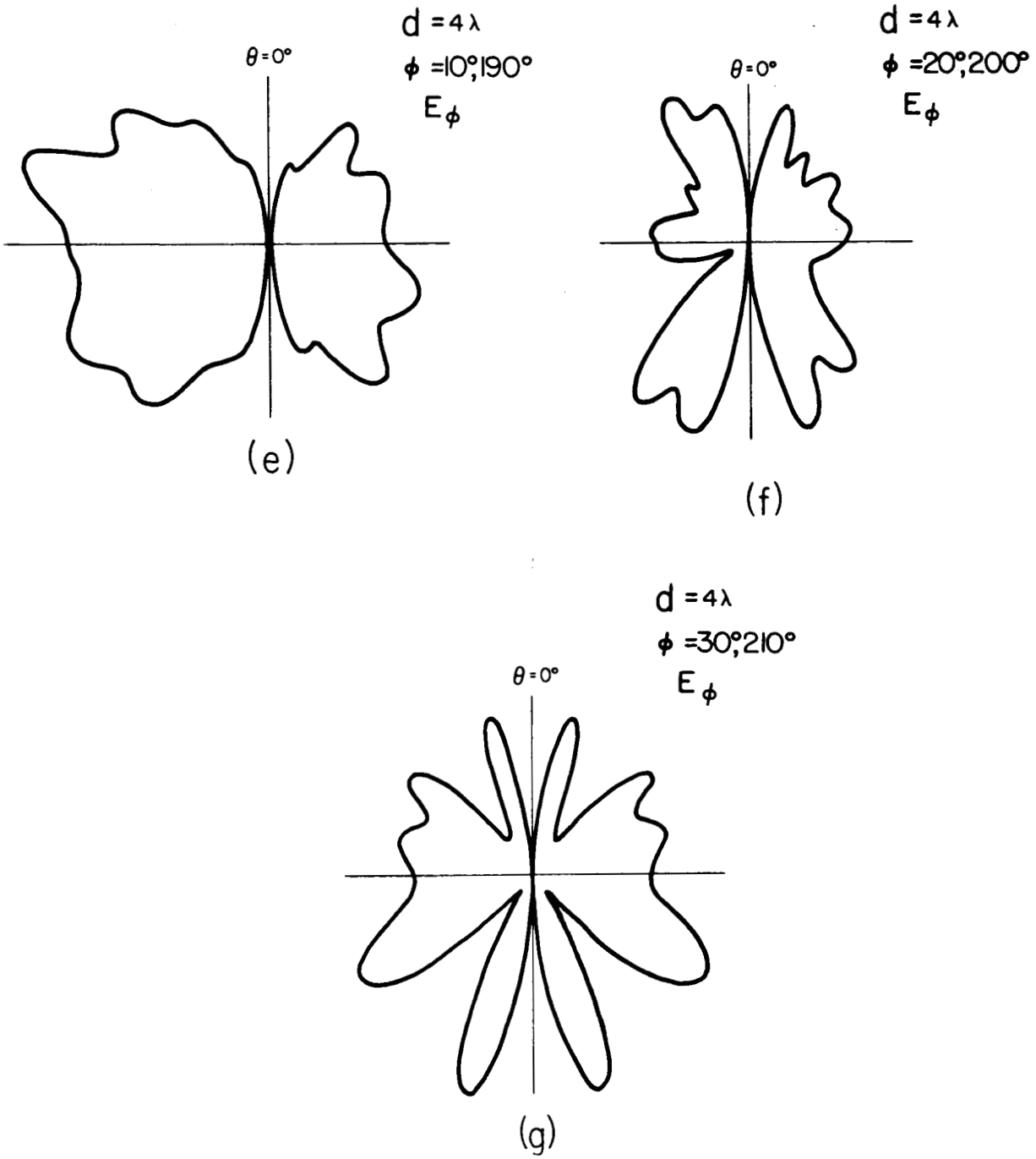

Fig. 10. Radiation patterns of four dipoles, symmetrically located and radially oriented on the surface of a sphere of diameter equal to 4λ.

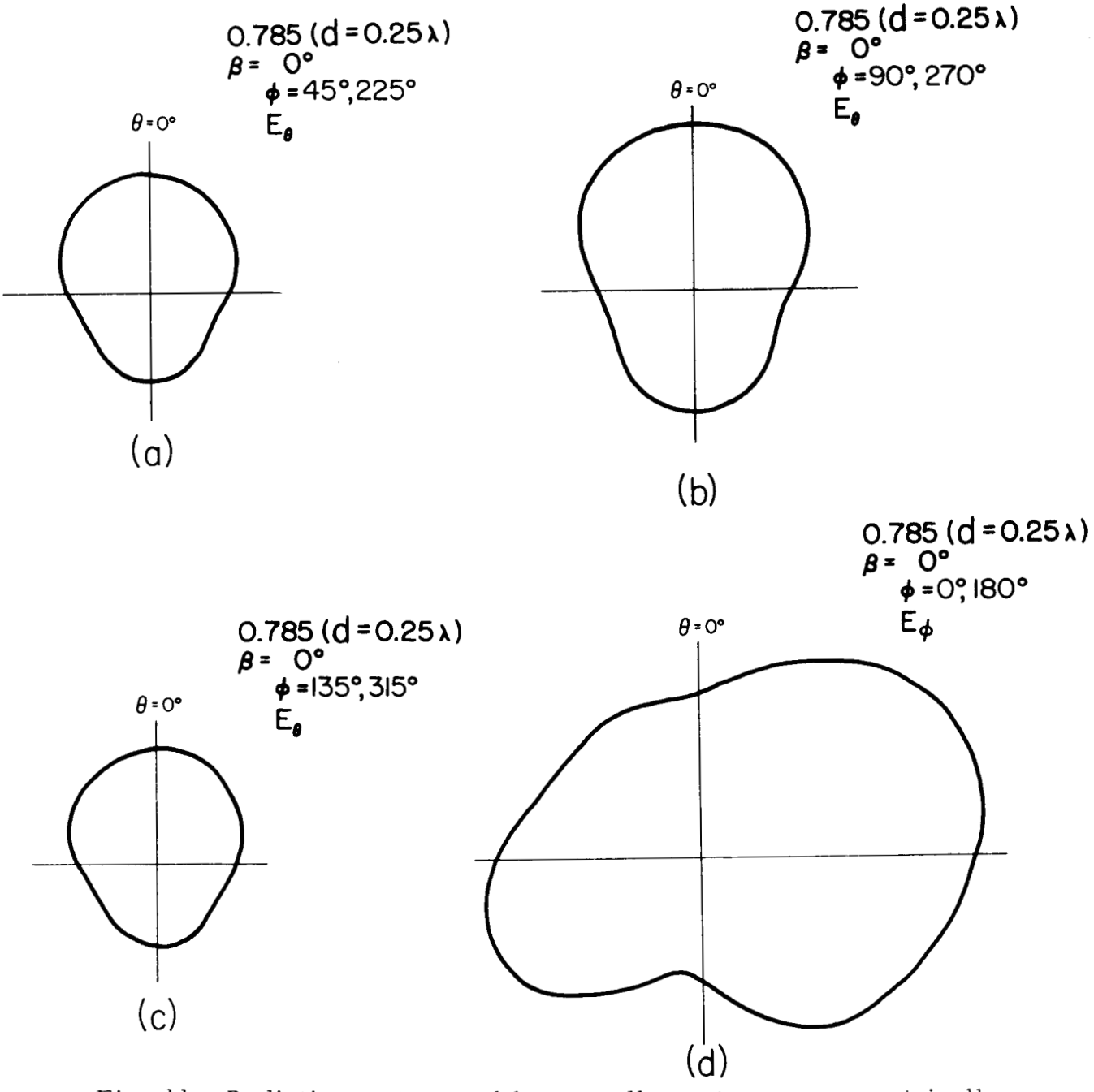

Fig. 11. Radiation patterns of four small apertures, symmetrically located on the surface of a sphere of diameter equal to 0.25λ, and with the field direction on the aperture the same as that of the unit vector $\hat{\phi}$.

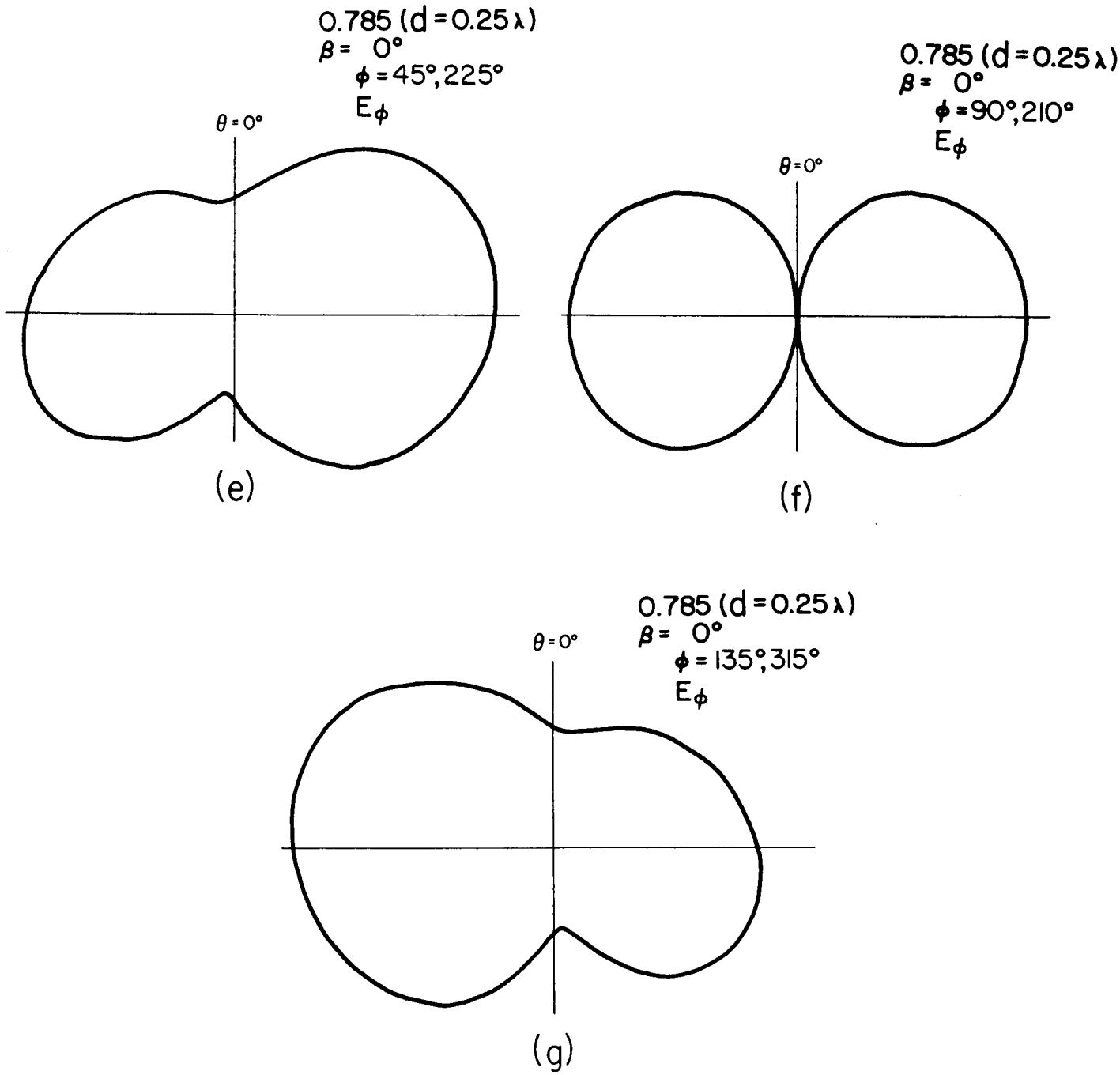

Fig. 11. Radiation patterns of four small apertures, symmetrically located on the surface of a sphere of diameter equal to 0.25λ, and with the field direction on the aperture the same as that of the unit vector $\hat{\phi}$.

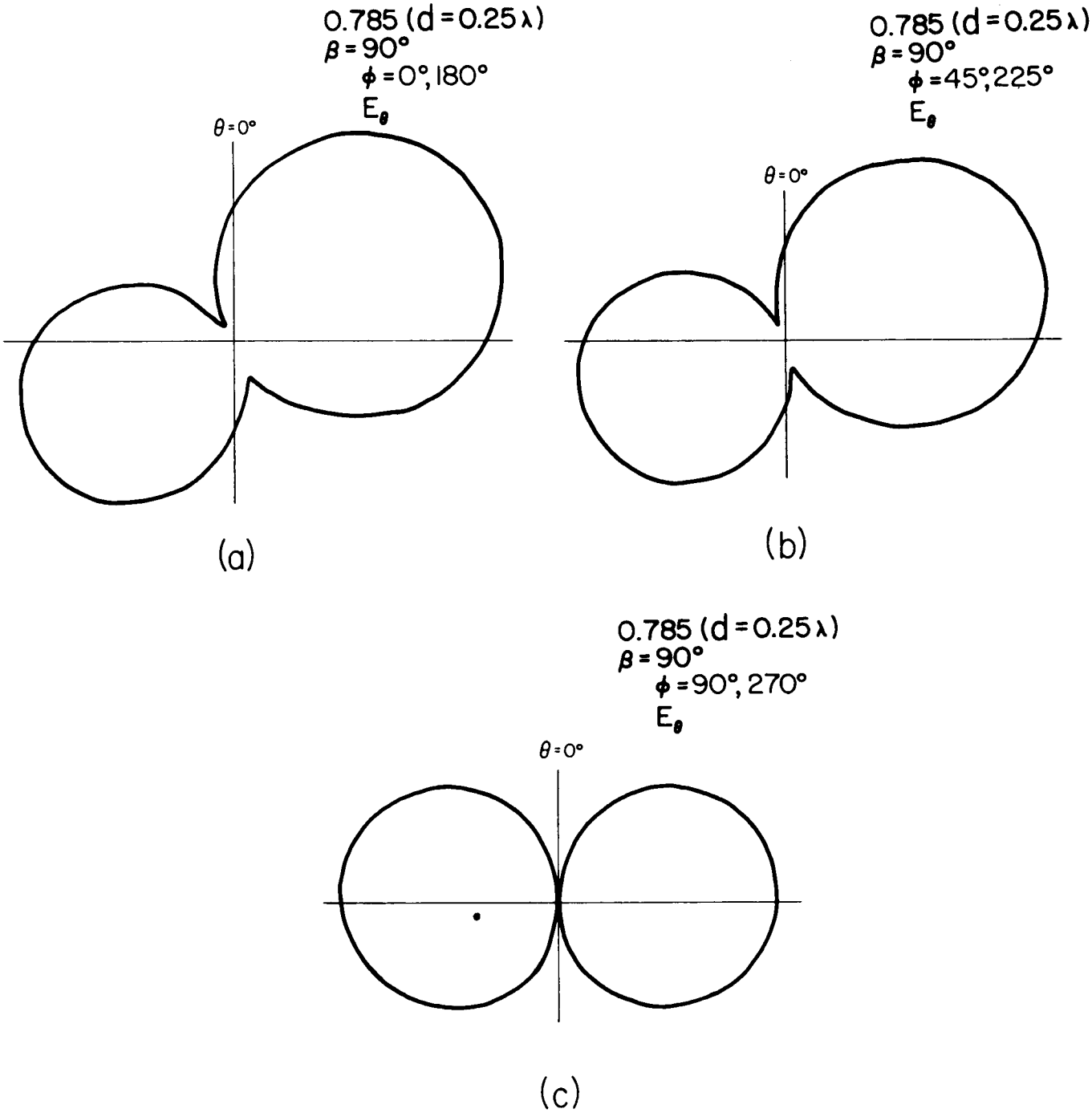

Fig. 12. Radiation patterns of four small apertures, symmetrically located on the surface of a sphere of diameter equal to 0.25λ, and with the field direction on the aperture perpendicular to the unit vector $\hat{\phi}$.

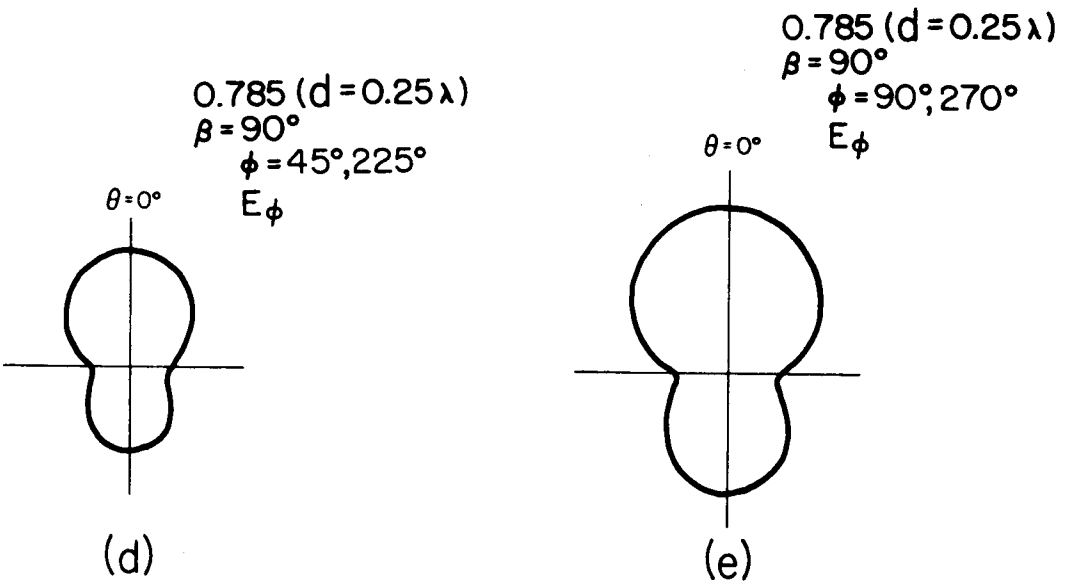

Fig. 12. Radiation patterns of four small apertures, symmetrically located on the surface of a sphere of diameter equal to 0.25λ, and with the field direction on the aperture perpendicular to the unit vector $\hat{\phi}$.

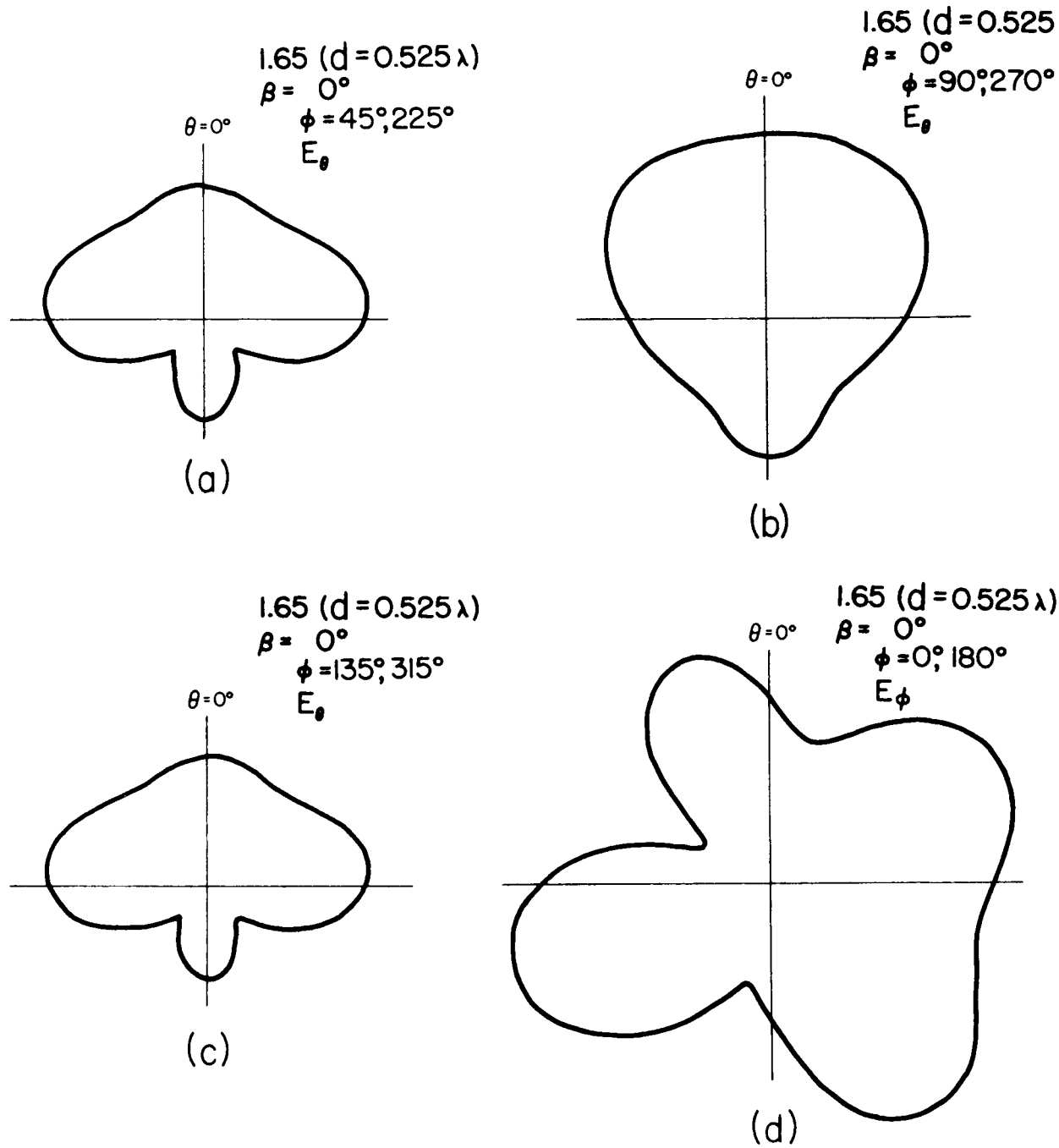

Fig. 13. Radiation patterns of four small apertures, symmetrically located on the surface of a sphere of diameter equal to 0.525λ, and with the field direction on the aperture the same as that of the unit vector $\hat{\phi}$.

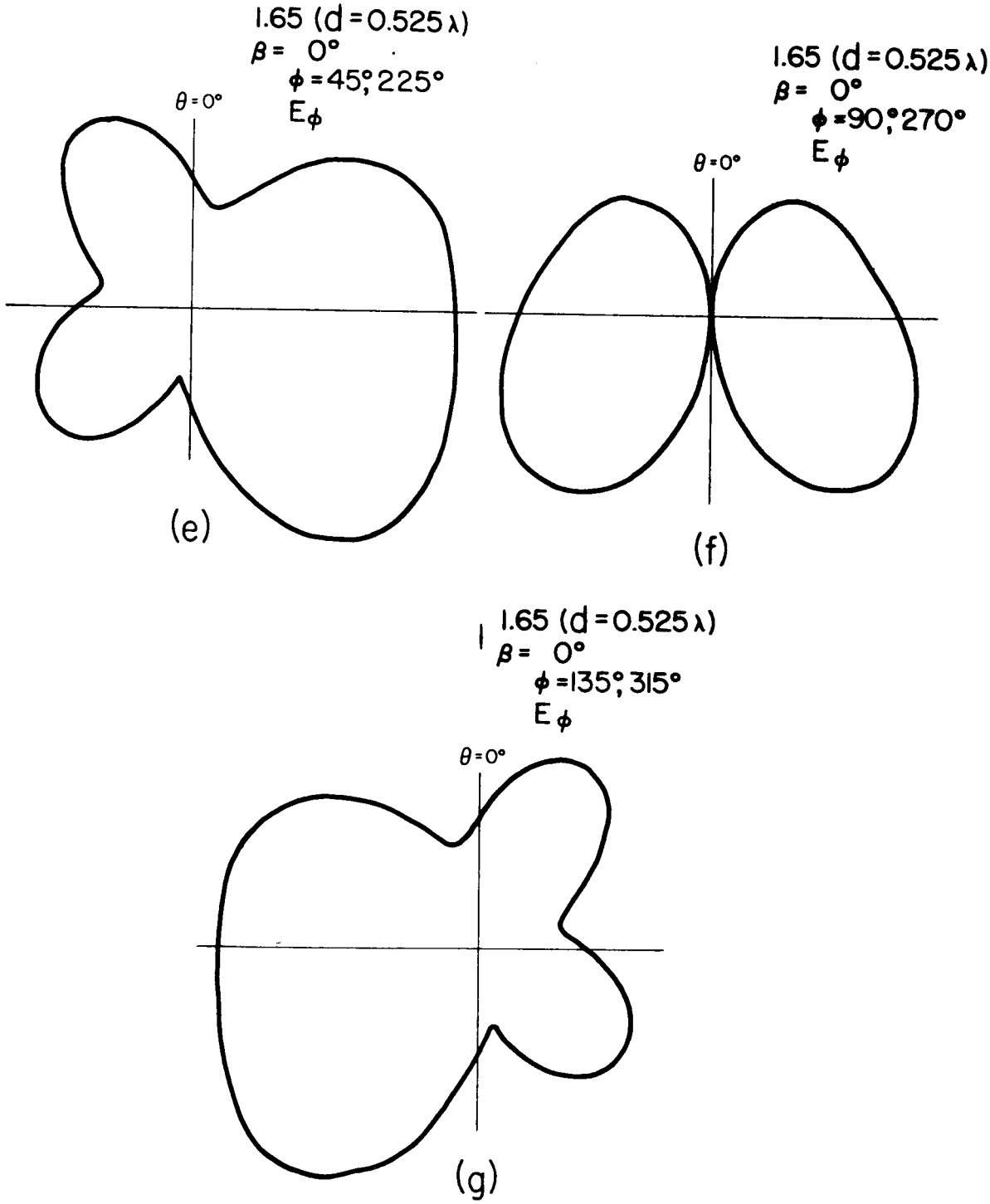

Fig. 13. Radiation patterns of four small apertures, symmetrically located on the surface of a sphere of diameter equal to 0.525λ, and with the field direction on the aperture the same as that of the unit vector $\hat{\phi}$.

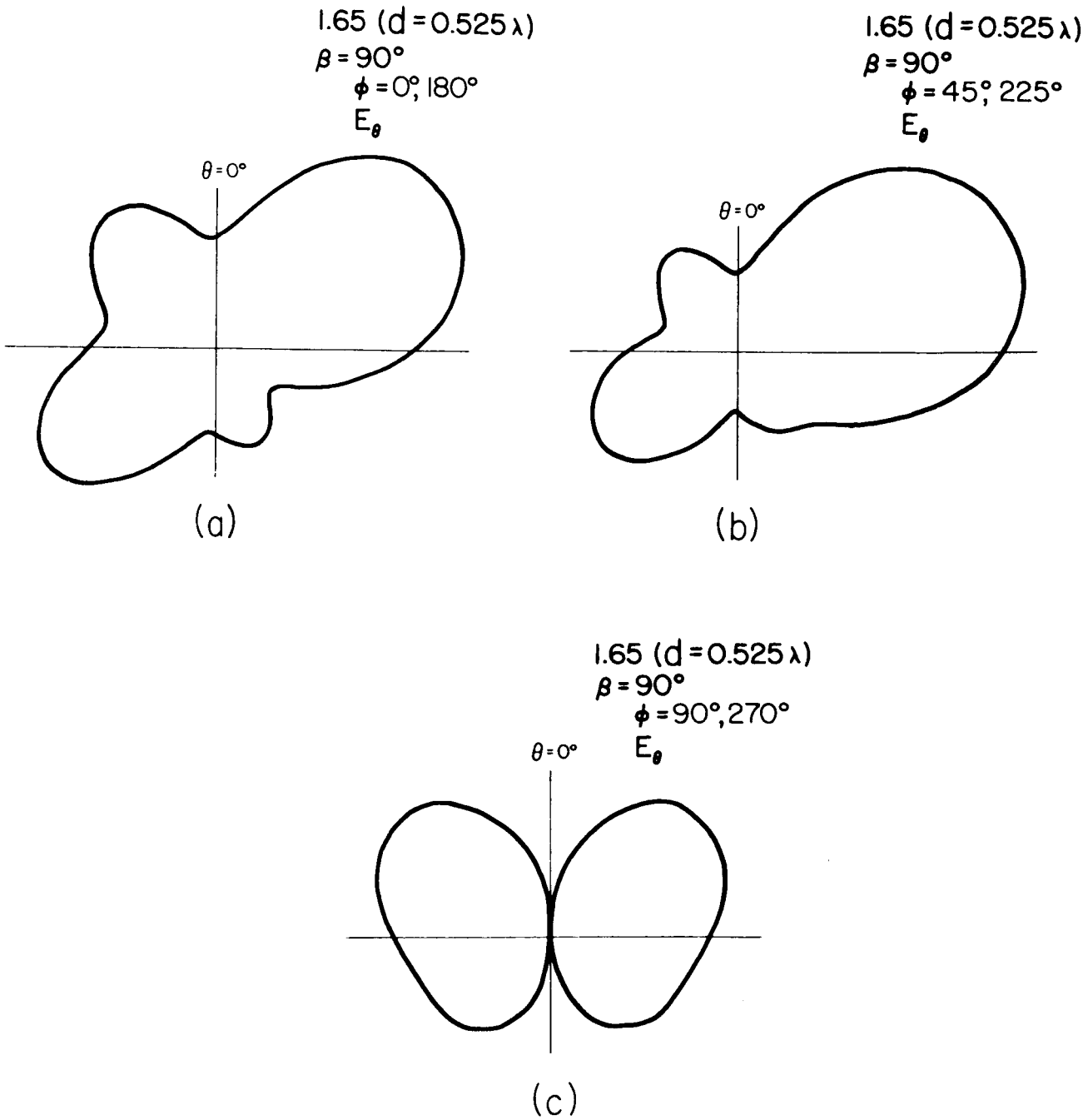

Fig. 14. Radiation patterns of four small apertures, symmetrically located on the surface of a sphere of diameter equal to 0.525λ, and with the field direction on the aperture perpendicular to the unit vector $\hat{\phi}$.

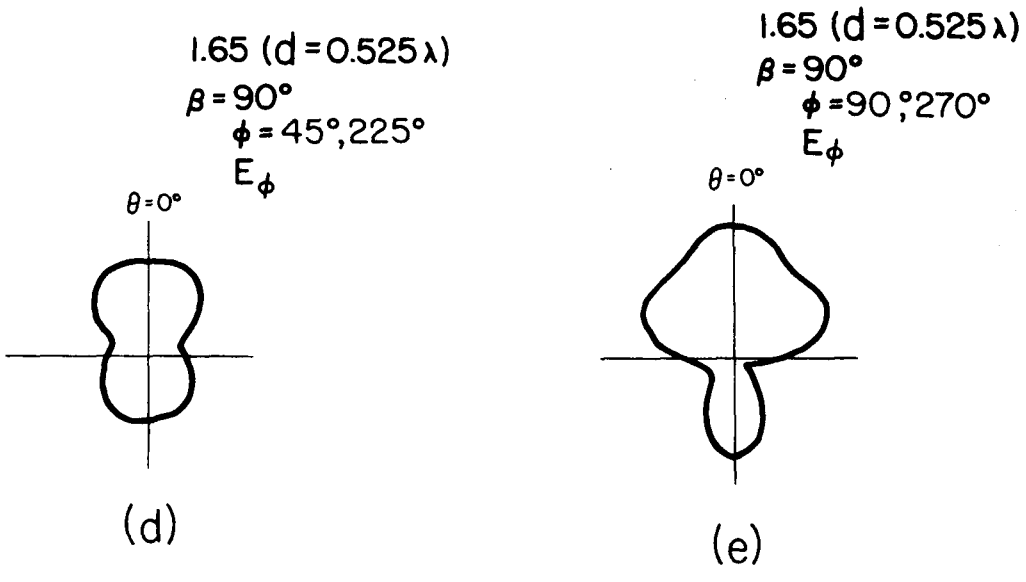

Fig. 14. Radiation patterns of four small apertures, symmetrically located on the surface of a sphere of diameter equal to 0.525λ, and with the field direction on the aperture perpendicular to the unit vector $\hat{\phi}$.

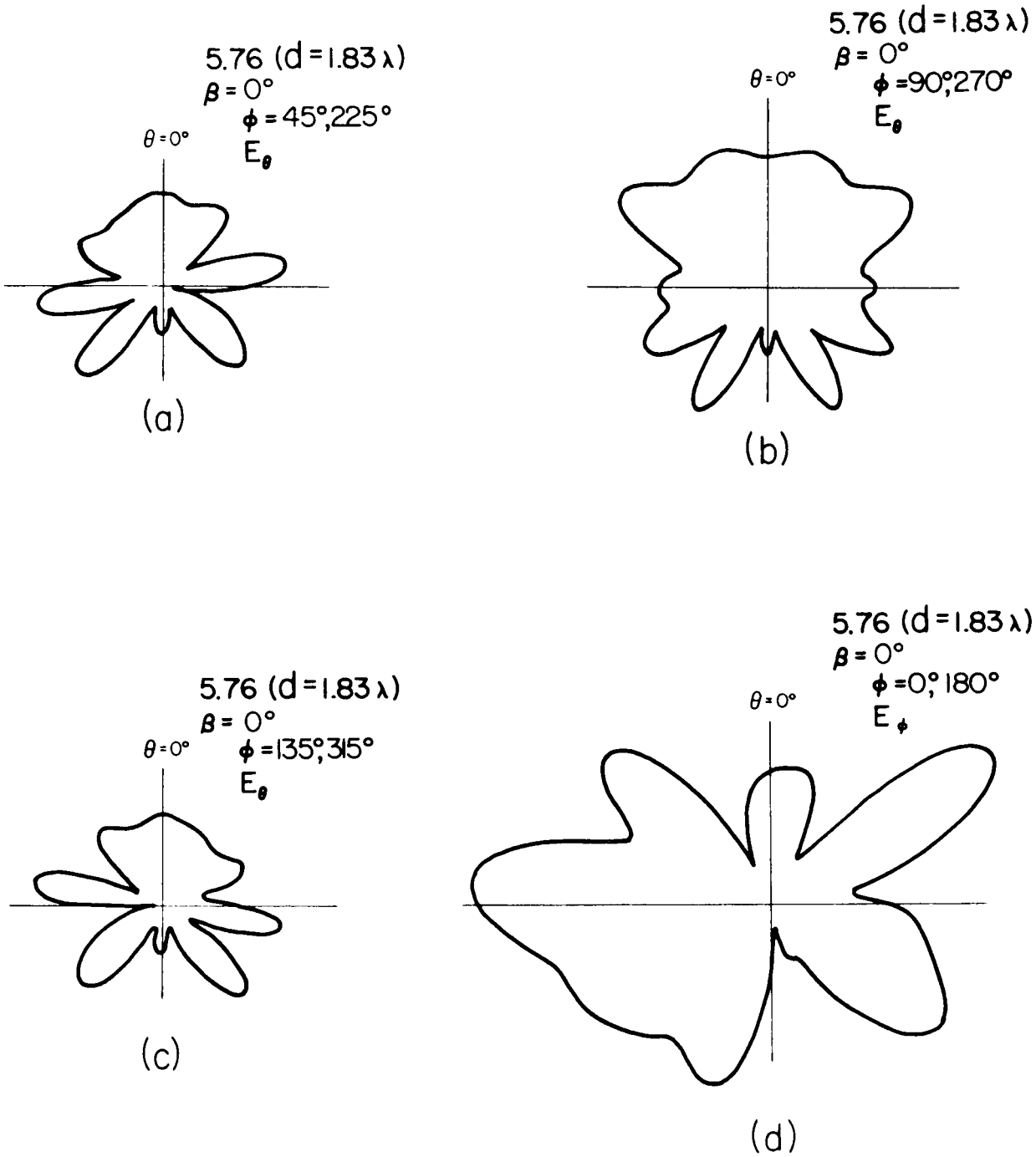

Fig. 15. Radiation patterns of four small apertures, symmetrically located on the surface of a sphere of diameter equal to 1.83λ, and with the field direction on the aperture the same as that of the unit vector $\hat{\phi}$.

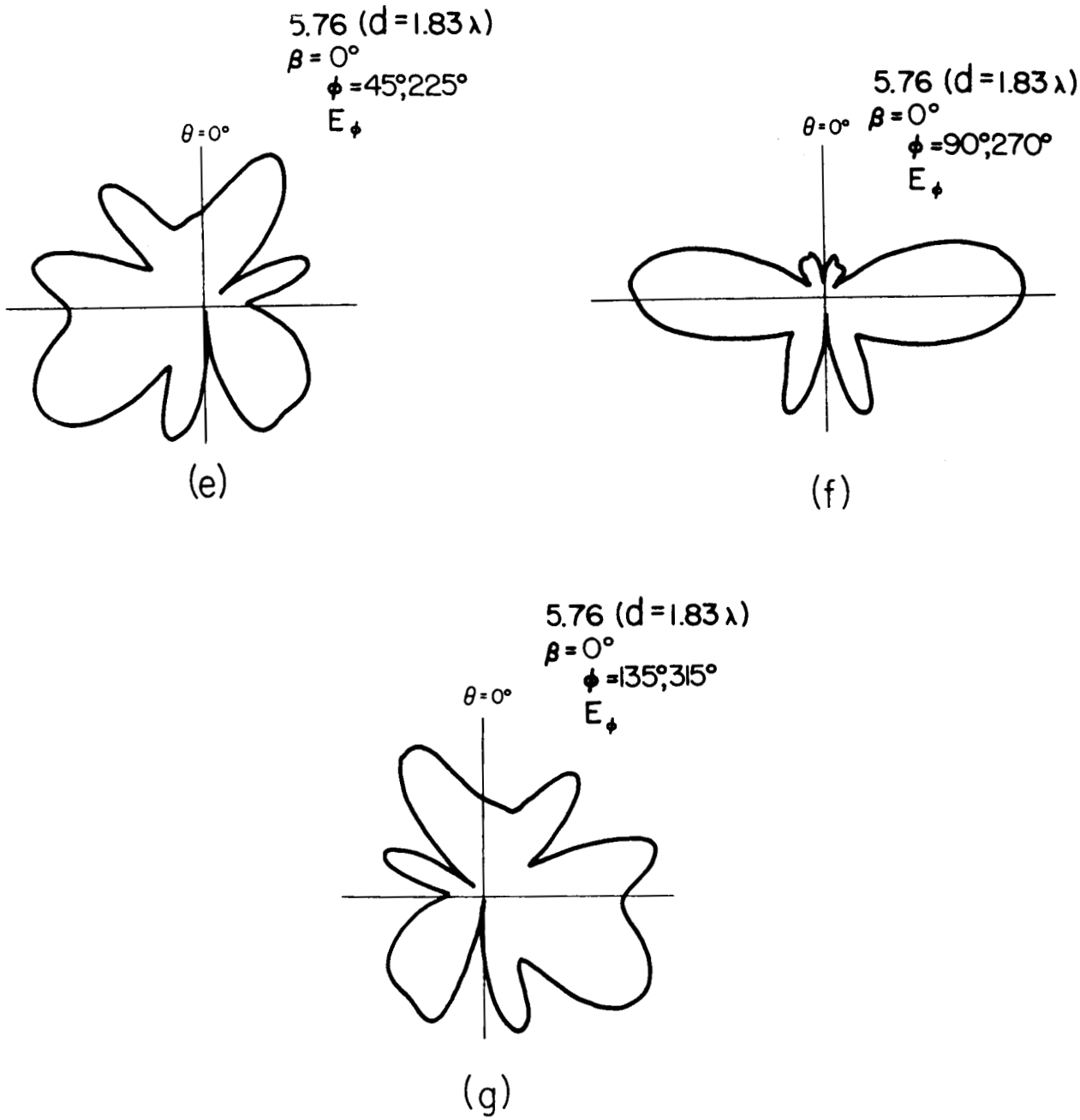

Fig. 15. Radiation patterns of four small apertures, symmetrically located on the surface of a sphere of diameter equal to 1.83λ, and with the field direction on the aperture the same as that of the unit vector $\hat{\phi}$.

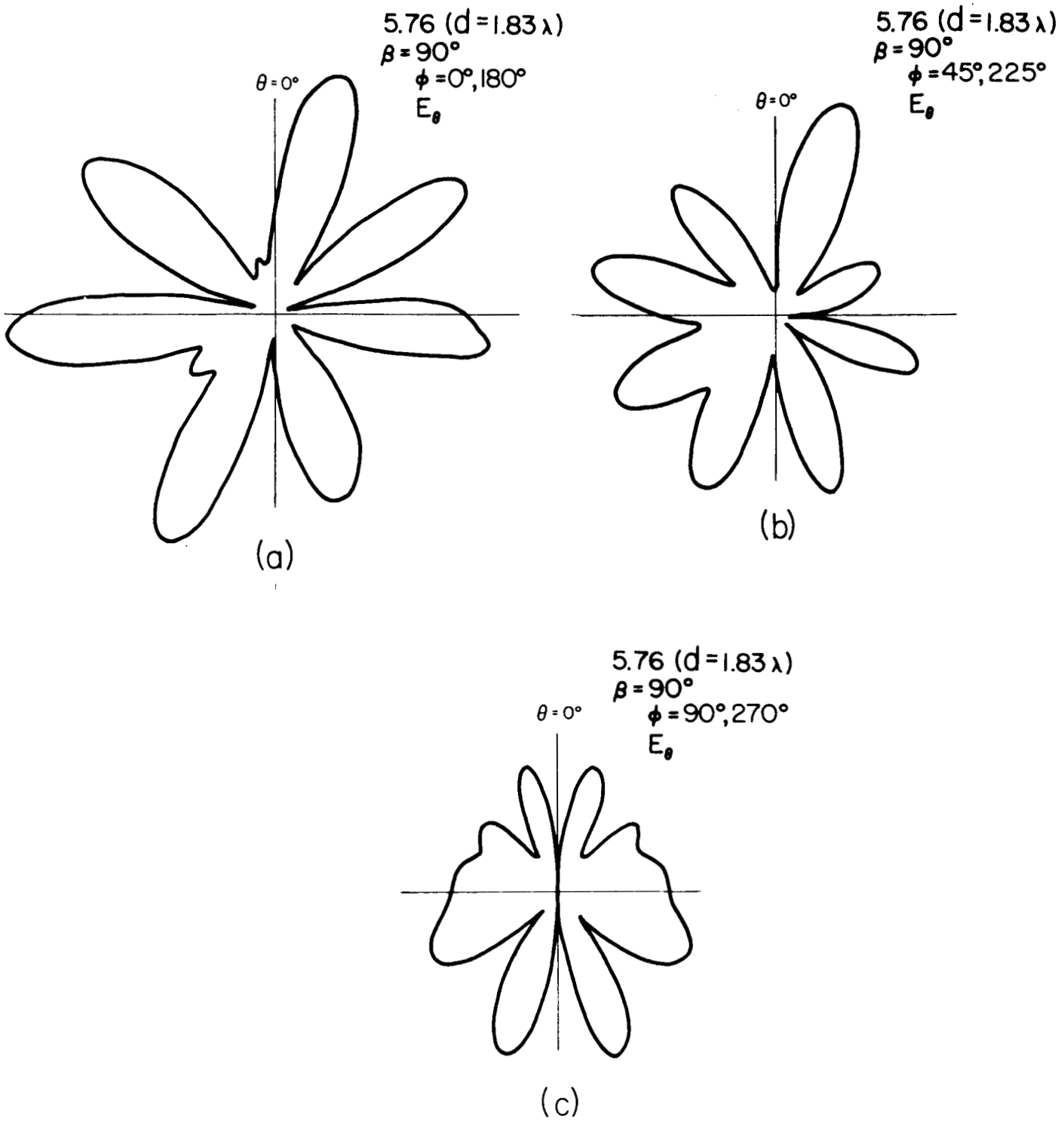

Fig. 16. Radiation patterns of four small apertures, symmetrically located on the surface of a sphere of diameter equal to 1.83λ, and with the field direction on the aperture perpendicular to the unit vector $\hat{\phi}$.

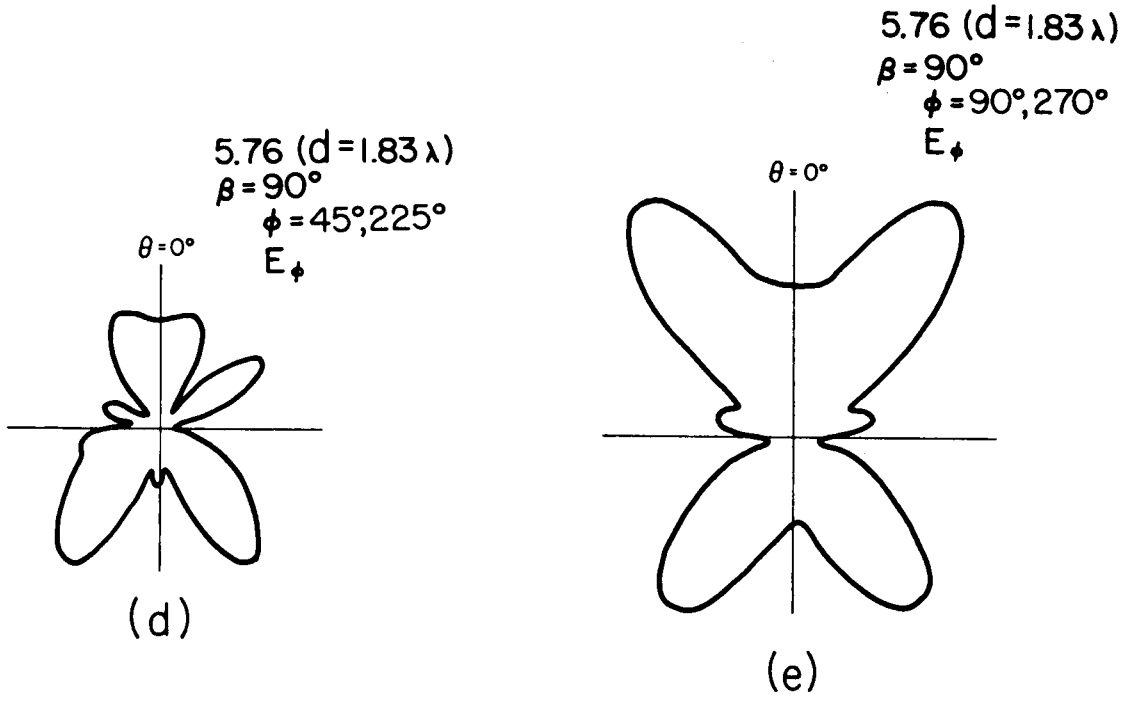

Fig. 16. Radiation patterns of four small apertures, symmetrically located on the surface of a sphere of diameter equal to 1.83λ, and with the field direction on the aperture perpendicular to the unit vector $\hat{\phi}$.

References

1. H. Levine and J. Schwinger, "On the Theory of Electromagnetic Wave Diffraction by an Aperture in an Infinite Plane Conducting Screen," Communications of Pure and Applied Mathematics III, 4, (1950), 355-391.

2. C.T. Tai, "A Glossary of Dyadic Green's Functions," Technical Report No. 46, Stanford Research Institute (July 19, 1954).

3. Fernado J. Corbato and Jack L. Uretsky, "Generation of Spherical Bessel Functions in Digital Computers," Journal of the Association for Computing Machinery 6, 3, July, 1959.